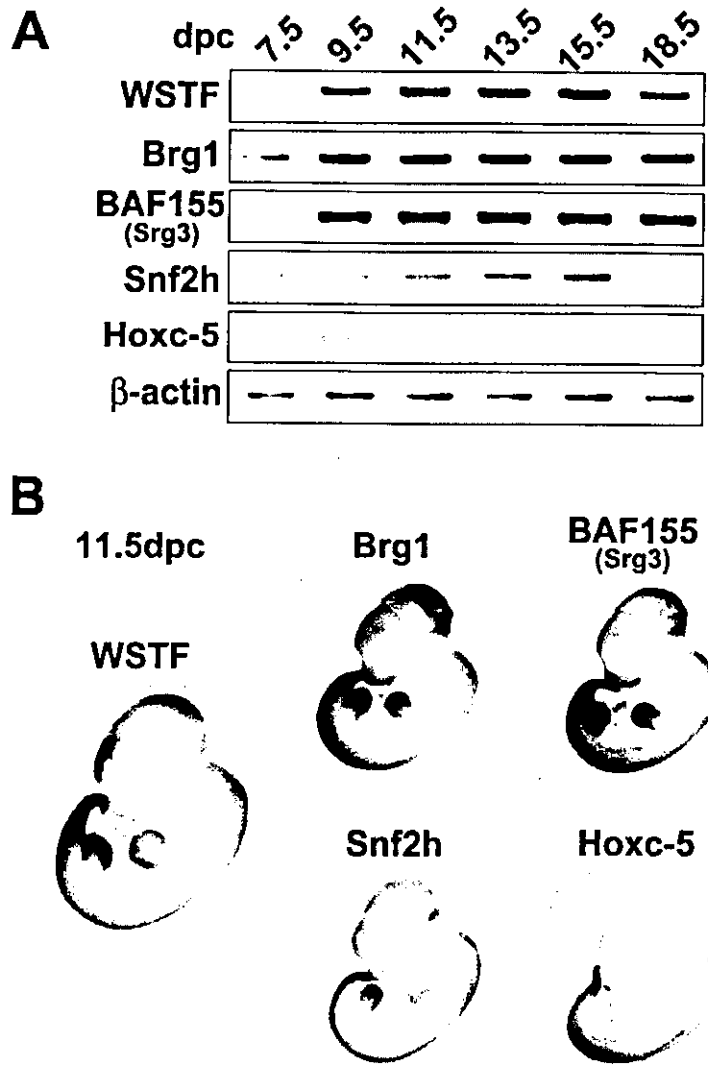

Figure 7. Spatiotemporal Expression Patterns of WSTF during Mouse Embryogenesis

(A) RT-PCR analysis of mouse WSTF, Brg1, BAF155 (Srg3), Snf2h, Hoxc-5, and β-actin gene expression. Embryos were dissected at the indicated times (7.5 dpc to 18.5 dpc). Samples were normalized by dilution to give equivalent signals for β-actin.

(B) Whole mount in situ hybridization analysis of mouse WSTF, Brg1, BAF155 (Srg3), Snf2h, and Hoxc-5 (negative control) expression at 11.5 dpc (Scale bar: 2 mm. Sense control probes were also hybridized and no signal was detected; data not shown).

WINAC subunit configuration is of interest to be clarified for defining the function of each component. A recent report has revealed that the chromatin-remodeling activity of the dISWI-based complex requires multiple Acf1 motifs to nonspecifically anchor DNA through its WAC motifs, and to directly interact with ISWI through the DDT domain (Fyodorov and Kadonaga, 2002). In addition to a core subunit role of WSTF, multiple functions as a pivotal factor to conduct the WINAC function could be further speculated from the conservation of several motifs that are shared with the other WAC family proteins, like hACF1 (Jones et al., 2000). Moreover, functions of the bromodomain and PHD finger motif in WSTF remain to be established in the promoter targeting and chromatin remodeling (Hassan et al., 2002; Schultz et al., 2002).

Promoter Targeting of VDR by WINAC and Cooperative WINAC Function with the Coregulator Complexes

Similar to the reported coactivator-like actions of the SWI2/SNF2 ATPases and BAF57 for the ligand-induced ERα transactivation (Chiba et al., 1994; DiRenzo et al., 2000; Belandia et al., 2002), overexpression of WSTF and the ATPase subunits as well could coactivate the ligand-induced VDR transactivation as either a GAL4 DBD chimeric protein or heterodimer with RXR (Figures 5A and 5C). VDR coactivation by the ligand-dependent NR coactivators (TIF2 and TRAP220) was abrogated by WSTF-RNAi expression (Figure 5A). However, neither such coactivator-like WSTF actions nor reduced coactivation by NR coactivators by the WSTF-RNAi expression was detected for ERα (Figure 5A) and the other receptors tested (data not shown), supporting the observed direct and selective interaction of WSTF with VDR among NRs (Figure 1D). Moreover, WSTF overexpression potentiated the ligand-induced transrepression of VDR on the 1α(OH)ase negative VDRE (Figure 5D), where an ablation of endogenous WSTF by RNAi expression led to a significant reduction in ligand-induced corepressor recruitment (lane 10 in Figure 5B). Thus, ligand-independent association of WINAC and VDR in the VDR target promoters appears to facilitate the local nucleosomal array

accessibility for ligand-dependent coregulators, following histone tail modifications by the recruited coregulator complexes (Hassan et al., 2002). It was recently reported that only when ligand is bound to ERα, all of the ERα p160/CBP HAT coactivator complex and human SWI/SNF-type complexes are targeted to the ER target promoters, although such ligand-induced occupancy of ERα and coregulator in the promoters appears in a cyclic fashion (Shang et al., 2000; Belandia et al., 2002). Such ligand-induced assembly of the SWI/SNF-type complexes with NRs through the p160/CBP complex might be a common mechanism for ligand-dependent targeting of NRs to the cognate promoters (Glass and Rosenfeld, 2000).

Unlike NRs such as ERα and AR (Belandia et al., 2002; Shang et al., 2002), VDR appears from ChIP analysis (Figure 5B) to be selectively targeted through WINAC to the promoters without ligand-induced activation of VDR function or following recruitment of coregulator complexes. WINAC targeting to the promoters appears not to require specific histone tail modifications by coregulators. Thus, it is likely that WINAC associating on promoters escort VDR for its recognition and specific binding to VDREs, through nucleosomal mobilization by WINAC, presumably cooperating with the other chromatin complexes (Lemon et al., 2001). Alternatively, once VDR happens to bind VDREs during nonspecific chromatin remodeling, WINAC might be acquired to VDR upon the promoters to engage in local nucleosome reorganization. The latter possibility coincides well with a recent report about a sequence-specific regulator, SATB1 (Yasui et al., 2002). As a result, the local chromatin structure near VDREs may transit into an active chromosomal state that appears competent for receipt of both the coactivator complexes and the corepressor complexes (Figures 5C and 5D) dependent on the VDRE sequences and the tertiary positions of DNA-bound VDR. This is not consistent with recent observations that the chromatin-remodeling complexes are recruited only after acetylation/deacetylation of histone tails by the coregulatory complexes (Hassan et al., 2002). However, the orders of the complex targetings are supposed to be dependent on the regulator type and the promoter context (Lomvardas and Thanos, 2002; Soutoglou and Talianidis, 2002).

Williams Syndrome Is a Chromatin-Remodeling Factor Disease?

We found that the ligand-induced transactivation function of VDR is impaired in the skin fibroblast cells of all three tested patients, in whom the regions covering the WSTF gene locus at the chromosome 7q11.23 are heterozygously deleted. Such impaired VDR function should not lead to severe defects in vitamin D actions in adults, since the adult VDR heterozygote mice ($VDR^{+/-}$) and the heterozygous carrier patients of the hereditary vitamin D-dependent type II rickets caused by VDR inactivation exhibited no overt abnormality in calcium and vitamin D metabolism, though VDR is a major regulator in those metabolisms (Yoshizawa et al., 1997). However, during growth, the mineral intakes must be greater than their excretions through the actions of calciotropic hormones, including vitamin D. It is tempting to speculate that the significantly reduced WINAC levels in WS patients transiently cause impaired function in VDR and other unidentified factors, leading to the transient appearance of infantile aberrant vitamin D metabolism and consequently, hypercalcemia (Taylor et al., 1982; Garabedian et al., 1985). These findings together suggest that a normal WSTF dose in the cells is necessary to support normal activities of VDR and presumably of some other regulators.

WSTF expression patterns during mouse embryogenesis overlap with those of the common components of WINAC (Bultman et al., 2000; Kim et al., 2001), but appear more limited. In contrast, the more restricted expression pattern was detected in mouse ISWI (Snf2h) (Lazzaro and Picketts, 2001) (Figure 7B). It is therefore possible to suggest that specific roles of WINAC among the other chromatin-remodeling complexes exert in a more spatiotemporal manner and support organogenesis of several selected tissues during embryogenesis through chromatin remodeling for, at least, transcription and DNA replication. Therefore, the WS patients may suffer a wide spectrum of disorders in certain organs. Thus, this study suggests that the Williams syndrome disorders are caused, at least in part, by WINAC dysfunction as a chromatin-remodeling disease.

Experimental Procedures

Plasmids and Antibodies

Chimeric GST proteins of GAL4 DBD (1–147 aa) fused with Rat VDR-DEF and WSTF deletion mutants were expressed in pGEX-2TK (Pharmacia Biotech). The promoter region of 1α,25-dihydroxyvitamin D3 24-hydroxylase (−367 to 0) and 25-hydroxyvitamin D3 1α-hydroxylase (−889 to −30) were inserted into the pGL3 vector (Promega) driven by a thymidine kinase (tk) promoter (Chen and DeLuca, 1995; Murayama et al., 1998; Yanagisawa et al., 2002). Rabbit polyclonal antipeptide antiserum was prepared by Sawady technology against KLQSEDSAKTEEVDEEKK, which is near the human WSTF C terminus.

Purification and Separation of VDR-Associated Complexes

For WINAC purification, the nuclear extracts of the MCF7 stable transformant were prepared by the same method as HeLa nuclear extracts (Rachez et al., 1998; Kitagawa et al., 2002; Yanagisawa et al., 2002). Then, they were bound to the GST column [GST], and 1α,25(OH)2D3-unbound GST-VDR column [GST-VDR(D3-)]. The complexes bound to the ligand-unbound VDR were eluted with 15 mM reduced glutathione in elution buffer (50 mM Tris-HCl [pH 8.3], 150 mM KCl, 0.5 mM EDTA, 0.5 mM PMSF, 5 mM NaF, 0.08% NP-40, 0.5 mg/ml BSA, and 10% glycerol). Next, they were layered on top of a 4.5 ml linear 100%–40% glycerol gradient in the GST binding buffer and centrifuged for 16 hr at 4°C at 40,000 rpm in a SW40 rotor (Beckman). Protein standards were ovalbumin (44 kDa), β-globulin (158 kDa), and thyroglobulin (667 kDa). Finally, the fractions containing WSTF and VDR were collected and loaded onto a 2.5–5 ml anti-FLAG M2 resin column (Sigma). After washing with binding buffer, the bound proteins were eluted by incubation for 60 min with 10–15 ml of the FLAG peptide (0.2 mg/ml) (Sigma) in binding buffer.

In Vitro Chromatin Reconstitution and Disruption Assay

Chromatin reconstitution and disruption reactions were performed essentially as previously described (Ito et al., 2000) using supercoiled plasmid DNA. A standard reaction contained plasmid (0.4 μg), purified core histones from *Drosophila* embryos (0.33 μg), purified recombinant dNAP1 (2.8 μg) [dNAP1], purified recombinant ACF (40 ng) [dACF], purified WINAC (100 ng) [WINAC], ATP (3 mM), and the ATP-regenerating system (30 mM phosphocreatine and 1mg/ml creatine phosphokinase). For the chromatin-disruption assay,

chromatin was reconstituted with DNA, pGIE0 (containing the GAL4 binding site) and purified histones by salt dialysis, and GST-GAL4 fusion proteins [e.g., GAL-VDR] mediated disruption of nucleosome arrays was analyzed by micrococcal nuclease digestion-Southern blot analysis.

In Vitro Transcription Assay

The purified proteins were purified as described previously (Ito et al., 2000). An in vitro transcription reactions and primer extension analysis was performed with pGI0 as an internal control, as previously described (Ito et al., 1997). Chromatin was reconstituted with DNA, pGIE0 (0.2 μg), and purified histones (0.24 μg) by salt dialysis and indicated purified GST-GAL4 fusion proteins (50 nM each final concentration), purified WINAC (50 ng) [WINAC] and p300 (40 nM) [p300] were added before the transcription reactions. After primer extension reactions, ^{32}P-labeled DNA was extracted by phenol-chroroform, precipitated by ethanol, analyzed on 8% acrylamide 8.3 M urea gels, and visualized by autoradiography.

In Vitro Replication Assay

An in vitro replication assay was performed as previously described (Ohba et al., 1996). Purified WINAC [WINAC], purified recombinant *Drosophila* NAP-1 [dNAP1], or *Drosophila* CAF-1 [dCAF1] was added before initiating the DNA replication reactions. The products were extracted and subjected to electrophoresis in a 1.5% agarose gel (1 × TBE) and visualized by autoradiography.

Cell Cycle Analysis Using RNAi and DNA Quantity Analysis

For immunoprecipitation during the double-thymidine treatment, about 80% of the confluent cells of FLAG-WSTF stable transformants were treated with thymidine (2.5 mM). After 24 hr, the cells were washed and cultured in normal medium for 10 hr (first release), then were treated with hydroxyurea (1 mM), and cultured for 16 hr (Fujita et al., 1996). Finally, the cells were washed and cultured in normal conditions (final release), then immunoprecipitated with anti-FLAG M2-resin. For the analysis of the DNA histogram, the FACS analysis was done using FACS Calibur (BD PharMingen) and CellQuest (BD PharMingen) (Fujita et al., 1996).

RNAi Experiments

The two short RNAs were transfected after they were annealed. The sequence of the indicated RNAi is as follows: WSTF-RNAi (5′-GAGUAUGAAGCCCGCUUGGTT-3′ and 5′-CCAAGCGGGCUUCAUAC-UCTT-3′); Brg1-RNAi (5′-CUCCUCGGCCAGGUCCUUCTT-3′ and 5′-GAA-GGACCUGGCCGAGGAGTT-3′); Brm-RNAi (5′-UUCUUGGGCCUAGUC-CAGGTT-3′ and 5′-CCUGGACUAGGCCCAAGAATT-3′); CAF-1 p150-RNAi (5′-UCUUGUCCCAAA-GGGGAAATT-3′ and 5′-UUUCCCCUUUGG-GACAAGATT-3′); and control-RNAi (5′-CAGUAAGUAGCCGGGAUGGTT-3′ and 5′-CCAUCCCGGCUACUUA-CUGTT-3′).

ChIP Assay

Preparation of soluble chromatin for PCR amplification was performed as previously reported (Shang et al., 2000; Yanagisawa et al., 2002). The primer pairs for 24(OH)ase were 5′-GGGAGGCGCGTTCGAA-3′ and 5′-TCCTATGCCCAG-GGAC-3′ (pVDRE) and 5′-CCTCCTTTGCACAAGG-TAGT-3′ and 5′-AATGCACGTAAAGCGGCA-AC-3′ (distal); the primers for 1a(OH)ase were 5′-ATTCCCATGTCTGGAAGGAG-3′ and 5′-CAGTGAGC-CCAGCCCCTTTA-3′ (nVDRE) and 5′-AAGCTTGTCTCAACCTCCTG-3′ and 5′-GTTCAGAGATTGTCTGTGGG-3′ (distal).

Acknowledgments

We thank Dr. Michael Jones for kindly providing the partial WSTF cDNAs; Dr. H. Kato and Dr. H. Iba for Brg1 and hBrm plasmids; Dr. J. Kadonaga for dNAP-1; Dr. C. Wu for dACF; Dr. J.K. Tyler for dCAF-1; and Drs. G. Mizuguchi and L. Freedman for technical discussion. We also thank Dr. K. Yamane, H. Kawano, and A. Unno for the technical support; Dr. L. Tora for the critical discussion; and Miss H. Higuchi for preparation of the manuscript. This work was supported in part by a grant-in-aid for priority areas from the Ministry of Education, Science, Sports, and Culture of Japan (S.K.).

Received: December 30, 2002
Revised: May 16, 2003
Accepted: May 28, 2003
Published: June 26, 2003

References

Belandia, B., Orford, R.L., Hurst, H.C., and Parker, M.G. (2002). Targeting of SWI/SNF chromatin remodelling complexes to estrogen-responsive genes. EMBO J. *21*, 4094–4103.

Bozhenok, L., Wade, P.A., and Varga-Weisz, P. (2002). WSTF-ISWI chromatin remodeling complex targets heterochromatic replication foci. EMBO J. *21*, 2231–2241.

Bultman, S., Gebuhr, T., Yee, D., La Mantia, C., Nicholson, J., Gilliam, A., Randazzo, F., Metzger, D., Chambon, P., Crabtree, G., and Magnuson, T. (2000). A Brg1 null mutation in the mouse reveals functional differences among mammalian SWI/SNF complexes. Mol. Cell *6*, 1287–1295.

Chen, K.S., and DeLuca, H.F. (1995). Cloning of the human 1 alpha,25-dihydroxyvitamin D-3 24-hydroxylase gene promoter and identification of two vitamin D-responsive elements. Biochim. Biophys. Acta *1263*, 1–9.

Chiba, H., Muramatsu, M., Nomoto, A., and Kato, H. (1994). Two human homologues of Saccharomyces cerevisiae SWI2/SNF2 and Drosophila brahma are transcriptional coactivators cooperating with the estrogen receptor and the retinoic acid receptor. Nucleic Acids Res. *22*, 1815–1820.

DiRenzo, J., Shang, Y., Phelan, M., Sif, S., Myers, M., Kingston, R., and Brown, M. (2000). BRG-1 is recruited to estrogen-responsive promoters and cooperates with factors involved in histone acetylation. Mol. Cell. Biol. *20*, 7541–7549.

Elbashir, S.M., Harborth, J., Lendeckel, W., Yalcin, A., Weber, K., and Tuschl, T. (2001). Duplexes of 21-nucleotide RNAs mediate RNA interference in cultured mammalian cells. Nature *411*, 494–498.

Emerson, B.M. (2002). Specificity of gene regulation. Cell *109*, 267–270.

Fujita, M., Kiyono, T., Hayashi, Y., and Ishibashi, M. (1996). hCDC47, a human member of the MCM family. Dissociation of the nucleus-bound form during S phase. J. Biol. Chem. *271*, 4349–4354.

Fyodorov, D.V., and Kadonaga, J.T. (2001). The many faces of chromatin remodeling: SWItching beyond transcription. Cell *106*, 523–525.

Fyodorov, D.V., and Kadonaga, J.T. (2002). Binding of Acf1 to DNA involves a WAC motif and is important for ACF-mediated chromatin assembly. Mol. Cell. Biol. *22*, 6344–6353.

Garabedian, M., Jacqz, E., Guillozo, H., Grimberg, R., Guillot, M., Gagnadoux, M.F., Broyer, M., Lenoir, G., and Balsan, S. (1985). Elevated plasma 1,25-dihydroxyvitamin D concentrations in infants with hypercalcemia and an elfin facies. N. Engl. J. Med. *312*, 948–952.

Glass, C.K., and Rosenfeld, M.G. (2000). The coregulator exchange in transcriptional functions of nuclear receptors. Genes Dev. *14*, 121–141.

Gu, W., Malik, S., Ito, M., Yuan, C.X., Fondell, J.D., Zhang, X., Martinez, E., Qin, J., and Roeder, R.G. (1999). A novel human SRB/MED-containing cofactor complex, SMCC, involved in transcription regulation. Mol. Cell *3*, 97–108.

Hassan, A.H., Prochasson, P., Neely, K.E., Galasinski, S.C., Chandy, M., Carrozza, M.J., and Workman, J.L. (2002). Function and selectivity of bromodomains in anchoring chromatin-modifying complexes to promoter nucleosomes. Cell *111*, 369–379.

Hoogenraad, C.C., Koekkoek, B., Akhmanova, A., Krugers, H., Dortland, B., Miedema, M., van Alphen, A., Kistler, W.M., Jaegle, M., Koutsourakis, M., et al. (2002). Targeted mutation of Cyln2 in the Williams syndrome critical region links CLIP-115 haploinsufficiency to neurodevelopmental abnormalities in mice. Nat. Genet. *32*, 116–127.

Ito, T., Bulger, M., Pazin, M.J., Kobayashi, R., and Kadonaga, J.T. (1997). ACF, an ISWI-containing and ATP-utilizing chromatin assembly and remodeling factor. Cell *90*, 145–155.

Ito, T., Ikehara, T., Nakagawa, T., Kraus, W.L., and Muramatsu, M. (2000). p300-mediated acetylation facilitates the transfer of histone H2A–H2B dimers from nucleosomes to a histone chaperone. Genes Dev. *14*, 1899–1907.

Jones, M.H., Hamana, N., Nezu, J., and Shimane, M. (2000). A novel family of bromodomain genes. Genomics *63*, 40–45.

Kamei, Y., Xu, L., Heinzel, T., Torchia, J., Kurokawa, R., Gloss, B., Lin, S.C., Heyman, R.A., Rose, D.W., Glass, C.K., and Rosenfeld, M.G. (1996). A CBP integrator complex mediates transcriptional activation and AP-1 inhibition by nuclear receptors. Cell *85*, 403–414.

Kim, J.K., Huh, S.O., Choi, H., Lee, K.S., Shin, D., Lee, C., Nam, J.S., Kim, H., Chung, H., Lee, H.W., et al. (2001). Srg3, a mouse homolog of yeast SWI3, is essential for early embryogenesis and involved in brain development. Mol. Cell. Biol. *21*, 7787–7795.

Kitagawa, H., Yanagisawa, J., Fuse, H., Ogawa, S., Yogiashi, Y., Okuno, A., Nagasawa, H., Nakajima, T., Matsumoto, T., and Kato, S. (2002). Ligand-selective potentiation of rat mineralocorticoid receptor activation function 1 by a CBP-containing histone acetyltransferase complex. Mol. Cell. Biol. *22*, 3698–3706.

Lazzaro, M.A., and Picketts, D.J. (2001). Cloning and characterization of the murine Imitation switch (ISWI) genes: differential expression patterns suggest distinct developmental roles for Snf2h and Snf2l. J. Neurochem. *77*, 1145–1156.

Lemon, B., Inouye, C., King, D.S., and Tjian, R. (2001). Selectivity of chromatin-remodelling cofactors for ligand-activated transcription. Nature *414*, 924–928.

LeRoy, G., Orphanides, G., Lane, W.S., and Reinberg, D. (1998). Requirement of RSF and FACT for transcription of chromatin templates in vitro. Science *282*, 1900–1904.

Lomvardas, S., and Thanos, D. (2002). Modifying gene expression programs by altering core promoter chromatin architecture. Cell *110*, 261–271.

Loyola, A., LeRoy, G., Wang, Y.H., and Reinberg, D. (2001). Reconstitution of recombinant chromatin establishes a requirement for histone-tail modifications during chromatin assembly and transcription. Genes Dev. *15*, 2837–2851.

Lu, X., Meng, X., Morris, C.A., and Keating, M.T. (1998). A novel human gene, WSTF, is deleted in Williams syndrome. Genomics *54*, 241–249.

Mangelsdorf, D.J., Thummel, C., Beato, M., Herrlich, P., Schutz, G., Umesono, K., Blumberg, B., Kastner, P., Mark, M., Chambon, P., et al. (1995). The nuclear receptor superfamily: the second decade. Cell *83*, 835–839.

Murayama, A., Takeyama, K., Kitanaka, S., Kodera, Y., Hosoya, T., and Kato, S. (1998). The promoter of the human 25-hydroxyvitamin D3 1 alpha-hydroxylase gene confers positive and negative responsiveness to PTH, calcitonin, and 1 alpha,25(OH)2D3. Biochem. Biophys. Res. Commun. *249*, 11–16.

Narlikar, G.J., Fan, H.Y., and Kingston, R.E. (2002). Cooperation between complexes that regulate chromatin structure and transcription. Cell *108*, 475–487.

Ohba, R., Matsumoto, K., and Ishimi, Y. (1996). Induction of DNA replication by transcription in the region upstream of the human c-myc gene in a model replication system. Mol. Cell. Biol. *16*, 5754–5763.

Onate, S.A., Tsai, S.Y., Tsai, M.J., and O'Malley, B.W. (1995). Sequence and characterization of a coactivator for the steroid hormone receptor superfamily. Science *270*, 1354–1357.

Peoples, R.J., Cisco, M.J., Kaplan, P., and Francke, U. (1998). Identification of the WBSCR9 gene, encoding a novel transcriptional regulator, in the Williams-Beuren syndrome deletion at 7q11.23. Cytogenet. Cell Genet. *82*, 238–246.

Poot, R.A., Dellaire, G., Hulsmann, B.B., Grimaldi, M.A., Corona, D.F., Becker, P.B., Bickmore, W.A., and Varga-Weisz, P.D. (2000). HuCHRAC, a human ISWI chromatin remodelling complex contains hACF1 and two novel histone-fold proteins. EMBO J. *19*, 3377–3387.

Rachez, C., Suldan, Z., Ward, J., Chang, C.P., Burakov, D., Erdjument-Bromage, H., Tempst, P., and Freedman, L.P. (1998). A novel protein complex that interacts with the vitamin D3 receptor in a ligand-dependent manner and enhances VDR transactivation in a cell-free system. Genes Dev. *12*, 1787–1800.

Schultz, D.C., Ayyanathan, K., Negorev, D., Maul, G.G., and Rauscher, F.J., 3rd. (2002). SETDB1: a novel KAP-1-associated histone H3, lysine 9-specific methyltransferase that contributes to HP1-mediated silencing of euchromatic genes by KRAB zinc-finger proteins. Genes Dev. *16*, 919–932.

Sekine, K., Ohuchi, H., Fujiwara, M., Yamasaki, M., Yoshizawa, T., Sato, T., Yagishita, N., Matsui, D., Koga, Y., Itoh, N., and Kato, S. (1999). Fgf10 is essential for limb and lung formation. Nat. Genet. *21*, 138–141.

Shang, Y., Hu, X., DiRenzo, J., Lazar, M.A., and Brown, M. (2000). Cofactor dynamics and sufficiency in estrogen receptor-regulated transcription. Cell *103*, 843–852.

Shang, Y., Myers, M., and Brown, M. (2002). Formation of the androgen receptor transcription complex. Mol. Cell *9*, 601–610.

Smith, S., and Stillman, B. (1989). Purification and characterization of CAF-I, a human cell factor required for chromatin assembly during DNA replication in vitro. Cell *58*, 15–25.

Soutoglou, E., and Talianidis, I. (2002). Coordination of PIC assembly and chromatin remodeling during differentiation-induced gene activation. Science *295*, 1901–1904.

Taylor, A.B., Stern, P.H., and Bell, N.H. (1982). Abnormal regulation of circulating 25-hydroxyvitamin D in the Williams syndrome. N. Engl. J. Med. *306*, 972–975.

Varga-Weisz, P.D., Wilm, M., Bonte, E., Dumas, K., Mann, M., and Becker, P.B. (1997). Chromatin-remodelling factor CHRAC contains the ATPases ISWI and topoisomerase II. Nature *388*, 598–602.

Yanagisawa, J., Kitagawa, H., Yanagida, M., Wada, O., Ogawa, S., Nakagomi, M., Oishi, H., Yamamoto, Y., Nagasawa, H., McMahon, S.B., et al. (2002). Nuclear receptor function requires a TFTC-type histone acetyl transferase complex. Mol. Cell *9*, 553–562.

Yasui, D., Miyano, M., Cai, S., Varga-Weisz, P., and Kohwi-Shigematsu, T. (2002). SATB1 targets chromatin remodelling to regulate genes over long distances. Nature *419*, 641–645.

Yoshizawa, T., Handa, Y., Uematsu, Y., Takeda, S., Sekine, K., Yoshihara, Y., Kawakami, T., Arioka, K., Sato, H., Uchiyama, Y., et al. (1997). Mice lacking the vitamin D receptor exhibit impaired bone formation, uterine hypoplasia and growth retardation after weaning. Nat. Genet. *16*, 391–396.

AC, Santa Cruz) for immunoprecipitation; a monoclonal antibody against haemagglutinin A (HA; 1867423, Roche), a polyclonal antibody against Myc (SC789, Santa Cruz), and antibodies against phosphylated (Ser 473) or total Akt (9270, New England Biolabs).

Statistical analysis

Results shown are the mean ± s.d. We analysed data by one-way analysis of variance (ANOVA). Individual statistical differences were determined by Scheffe's multiple range comparison test.

Accession numbers

The sequences of mouse and human ERas can be retrieved from DDBJ/GenBank/EMBL with accession numbers AB093573 and AB093575.

Received 10 February; accepted 1 April 2003; doi:10.1038/nature01646.

1. Evans, M. J. & Kaufman, M. H. Establishment in culture of pluripotential cells from mouse embryos. *Nature* **292**, 154–156 (1981).
2. Martin, G. R. Isolation of a pluripotent cell line from early mouse embryos cultured in medium conditioned by teratocarcinoma stem cells. *Proc. Natl Acad. Sci. USA* **78**, 7634–7638 (1981).
3. Thomson, J. A. *et al.* Embryonic stem cell lines derived from human blastocysts. *Science* **282**, 1145–1147 (1998).
4. Freed, C. R. Will embryonic stem cells be a useful source of dopamine neurons for transplant into patients with Parkinson's disease? *Proc. Natl Acad. Sci. USA* **99**, 1755–1757 (2002).
5. Seeburg, P. H., Colby, W. W., Capon, D. J., Goeddel, D. V. & Levinson, A. D. Biological properties of human *c-Ha-ras1* genes mutated at codon 12. *Nature* **312**, 71–75 (1984).
6. Rodriguez-Viciana, P. *et al.* Phosphatidylinositol-3-OH kinase as a direct target of Ras. *Nature* **370**, 527–532 (1994).
7. Moodie, S. A., Willumsen, B. M., Weber, M. J. & Wolfman, A. Complexes of Ras.GTP with Raf-1 and mitogen-activated protein kinase kinase. *Science* **260**, 1658–1661 (1993).
8. Zhang, X. P. *et al.* Normal and oncogenic $p21^{ras}$ proteins bind to the amino-terminal regulatory domain of c-Raf-1. *Nature* **364**, 308–313 (1993).
9. Takai, Y., Sasaki, T. & Matozaki, T. Small GTP-binding proteins. *Physiol. Rev.* **81**, 153–208 (2001).
10. Chen, Z. Q., Ulsh, L. S., DuBois, G. & Shih, T. Y. Posttranslational processing of p21 ras proteins involves palmitylation of the C-terminal tetrapeptide containing cysteine-186. *J. Virol.* **56**, 607–612 (1985).
11. Willumsen, B. M., Christensen, A., Hubbert, N. L., Papageorge, A. G. & Lowy, D. R. The p21 ras C-terminus is required for transformation and membrane association. *Nature* **310**, 583–586 (1984).
12. Miyoshi, J., Kagimoto, M., Soeda, E. & Sakaki, Y. The human *c-Ha-ras2* is a processed pseudogene inactivated by numerous base substitutions. *Nucleic Acids Res.* **12**, 1821–1828 (1984).
13. Meiner, V. L. *et al.* Disruption of the acyl-CoA:cholesterol acyltransferase gene in mice: evidence suggesting multiple cholesterol esterification enzymes in mammals. *Proc. Natl Acad. Sci. USA* **93**, 14041–14046 (1996).
14. Li, E., Bestor, T. H. & Jaenisch, R. Targeted mutation of the DNA methyltransferase gene results in embryonic lethality. *Cell* **69**, 915–926 (1992).
15. Nichols, J., Evans, E. P. & Smith, A. G. Establishment of germ-line-competent embryonic stem (ES) cells using differentiation inhibiting activity. *Development* **110**, 1341–1348 (1990).
16. Gassmann, M., Donoho, G. & Berg, P. Maintenance of an extrachromosomal plasmid vector in mouse embryonic stem cells. *Proc. Natl Acad. Sci. USA* **92**, 1292–1296 (1995).
17. Pasano, O. *et al.* Analysis of the transforming potential of the human H-ras gene by random mutagenesis. *Proc. Natl Acad. Sci. USA* **81**, 4008–4012 (1984).
18. Serrano, M., Lin, A. W., McCurrach, M. E., Beach, D. & Lowe, S. W. Oncogenic *ras* provokes premature cell senescence associated with accumulation of p53 and $p16^{INK4a}$. *Cell* **88**, 593–602 (1997).
19. Cheng, A. M. *et al.* Mammalian Grb2 regulates multiple steps in embryonic development and malignant transformation. *Cell* **95**, 793–803 (1998).
20. Burdon, T., Stracey, C., Chambers, I., Nichols, J. & Smith, A. Suppression of SHP-2 and ERK signalling promotes self-renewal of mouse embryonic stem cells. *Dev. Biol.* **210**, 30–43 (1999).
21. Rodriguez-Viciana, P. *et al.* Role of phosphoinositide 3-OH kinase in cell transformation and control of the actin cytoskeleton by Ras. *Cell* **89**, 457–467 (1997).
22. Di Cristofano, A., Pesce, B., Cordon-Cardo, C. & Pandolfi, P. P. Pten is essential for embryonic development and tumour suppression. *Nature Genet.* **19**, 348–355 (1998).
23. Sun, H. *et al.* PTEN modulates cell cycle progression and cell survival by regulating phosphatidylinositol 3,4,5-trisphosphate and Akt/protein kinase B signaling pathway. *Proc. Natl Acad. Sci. USA* **96**, 6199–6204 (1999).
24. Burgering, B. M. & Coffer, P. J. Protein kinase B (c-Akt) in phosphatidylinositol-3-OH kinase signal transduction. *Nature* **376**, 599–602 (1995).
25. Franke, T. F. *et al.* The protein kinase encoded by the Akt proto-oncogene is a target of the PDGF-activated phosphatidylinositol 3-kinase. *Cell* **81**, 727–736 (1995).
26. Klippel, A. *et al.* Membrane localization of phosphatidylinositol 3-kinase is sufficient to activate multiple signal-transducing kinase pathways. *Mol. Cell. Biol.* **16**, 4117–4127 (1996).
27. Jirmanova, L., Afanassieff, M., Gobert-Gosse, S., Markossian, S. & Savatier, P. Differential contributions of ERK and PI3-kinase to the regulation of cyclin D1 expression and to the control of the G1/S transition in mouse embryonic stem cells. *Oncogene* **21**, 5515–5528 (2002).
28. Quilliam, L. A. M.-R. *et al.* Rap/R-Ras3, a transforming ras protein regulated by Sos1, GRF1, and p120 Ras GTPase-activating protein, interacts with the putative Ras effector AF6. *J. Biol. Chem.* **274**, 23850–23857 (1999).
29. Clark, G. J., Cox, A. D., Graham, S. M. & Der, C. J. Biological assays for Ras transformation. *Methods Enzymol.* **255**, 395–412 (1995).
30. Rosario, M., Paterson, H. F. & Marshall, C. J. Activation of the Raf/MAP kinase cascade by the Ras-related protein TC21 is required for the TC21-mediated transformation of NIH 3T3 cells. *EMBO J.* **18**, 1270–1279 (1999).

Supplementary Information accompanies the paper on **www.nature.com/nature.**

Acknowledgements We thank E. Kaiho, Y. Tokuzawa and M. Murakami for discussion; C. Takigawa and J. Iida for technical assistance; T. Ichisaka and Y. Samitsu for blastocyst microinjection; R. Farese Jr for RF8 ES cells, R. Jaenisch and T. Noda for J1 cells; W. Skarnes and S. Young for CGR8 cells; H. Niwa for MG1.19 cells, pCAG-IP and pBIKS(−)BgeopA; M. Okabe and J.-i. Miyazaki for pCX–EGFP; K. Kohno and T. Kitamura for PLAT-E cells and pMX retroviral vectors; and S. Young, R. Farese Jr and R. Pitas for critically reading the manuscript.

Competing interests statement The authors declare that they have no competing financial interests.

Correspondence and requests for materials should be addressed to S.Y. (shinyay@gtc.aist-nara.ac.jp).

Modulation of oestrogen receptor signalling by association with the activated dioxin receptor

Fumiaki Ohtake*, Ken-ichi Takeyama*†, Takahiro Matsumoto*, Hirochika Kitagawa*, Yasuji Yamamoto‡, Keiko Nohara§‖, Chiharu Tohyama§‖, Andree Krust¶, Junsei Mimura‖#, Pierre Chambon¶, Junn Yanagisawa*†, Yoshiaki Fujii-Kuriyama‖# & Shigeaki Kato*†

* *The Institute of Molecular and Cellular Biosciences, University of Tokyo, 1-1-1 Yayoi, Bunkyo-ku, Tokyo, 113-0032, Japan*
† *SORST, Japan Science and Technology, Kawaguchi, Saitama 332-0012, Japan*
‡ *Taiho Pharmaceutical Company Ltd, Cancer Research Laboratory, Hanno Research Center, Hanno, Saitama, 357-8527, Japan*
§ *National Institute for Environmental Studies, Tsukuba, Ibaraki 305-8506, Japan*
‖ *CREST, Japan Science and Technology, Kawaguchi, Saitama 332-0012, Japan*
¶ *Institut de Génétique et de Biologie Moleculaire et Cellulaire, CNRS, INSERM, Université Louis Pasteur, Collège de France, 67404 Illkirch, Strasbourg, France*
\# *TARA Center, University of Tsukuba, Tennodai, Tsukuba, 305-8577, Japan*

Environmental contaminants affect a wide variety of biological events in many species. Dioxins are typical environmental contaminants that exert adverse oestrogen-related effects[1]. Although their anti-oestrogenic actions[2,3] are well described, dioxins can also induce endometriosis[4–7] and oestrogen-dependent tumours[8,9], implying possible oestrogenic effects. However, the molecular mechanism underlying oestrogen-related actions of dioxins remains largely unknown. A heterodimer of the dioxin receptor (AhR) and Arnt, which are basic helix–loop–helix/PAS-family transcription factors, mediates most of the toxic effects of dioxins[10,11]. Here we show that the agonist-activated AhR/Arnt heterodimer directly associates with oestrogen receptors ER-α and ER-β. This association results in the recruitment of unliganded ER and the co-activator p300 to oestrogen-responsive gene promoters, leading to activation of transcription and oestrogenic effects. The function of liganded ER is attenuated. Oestrogenic actions of AhR agonists were detected in wild-type ovariectomized mouse uteri, but were absent in $AhR^{-/-}$ or $ER\text{-}\alpha^{-/-}$ ovariectomized mice. Our findings suggest a novel mechanism by which ER-mediated oestrogen signalling is modulated by a co-regulatory-like function of activated AhR/Arnt, giving rise to adverse oestrogen-related actions of dioxin-type environmental contaminants.

ERs, which are members of the nuclear receptor (NR) family[12,13], and AhR/Arnt are both ligand-dependent transcription factors. Ligand-activated AhR heterodimerizes with Arnt and activates the transcription of dioxin target genes such as *CYP1A1* (refs 10,11) through xenobiotic response elements (XREs). ERs bind to oestrogen response elements (EREs) and activate transcription in an oestrogen-dependent manner. This transcriptional activation

requires the recruitment of co-activator complexes[13–18], including histone acetyltransferase (HAT) complexes containing p300 and CREB binding protein (CBP). In view of previous reports that AhR ligands exhibit oestrogen-related adverse effects, it is possible that ER-mediated oestrogen signalling might cross-talk with AhR-mediated signalling through an unknown mechanism that regulates transcription. We therefore decided to examine whether AhR/Arnt heterodimer could transcriptionally affect ER transactivation functions, thereby modulating oestrogen signalling.

To monitor the transactivation function of endogenous receptors, luciferase reporter plasmids bearing consensus binding elements—ERE for ERs, and XRE for AhR/Arnt—were transfected into MCF-7 cells, a breast cancer cell line known to express both receptors endogenously[2]. Although the synthetic AhR ligand 3-methylcholanthrene (3MC) effectively activated transcription through XRE[10], 17β-estradiol (E2) did not, as expected (Fig. 1a). However, to our surprise, 3MC alone activated ERE-mediated transcription in the absence of E2 (Fig. 1a). In the presence of E2, ERE-mediated transcription was decreased by the addition of 3MC. Western blotting showed that the amount of ligand-induced transactivation did not simply reflect variations in receptor numbers (Fig. 1a). 3MC alone decreased AhR and ER-α protein levels, in agreement with previous reports[19].

We then examined the effect of AhR/Arnt on ER-mediated transcription by using exogenous receptors in Ishikawa cells, a uterine tumour cell line. Again, 3MC potently stimulated ERE-mediated transcription in the absence of E2 when both ER (either ER-α or ER-β) and AhR/Arnt were expressed, whereas it lowered the E2-induced transactivation function of ERs (Fig. 1b) without binding directly to ERs (Supplementary Fig. 1a) or affecting expression levels of ERs (data not shown). This activation effect of 3MC requires ERE (Fig. 1b, lanes 1–4), ER-α (lanes 7 and 8), AhR (lanes 9 and 10) and Arnt (lanes 11 and 12). To verify that an AhR ligand does indeed exert oestrogenic action through direct binding to AhR, other AhR ligands were further tested. More stable ligands such as 2,3,7,8-tetrachlorodibenzo-*p*-dioxin (TCDD), benzo[*a*]-pyrene and β-naphthoflavone acted as agonists, like 3MC (Fig. 1c), whereas the oestrogenic action of 3MC was blocked by either a known AhR antagonist, α-naphthoflavone or a pure oestrogen antagonist, ICI182,780 (Fig. 1d). The modulation of transcription activity by AhR/Arnt observed with ERs was not detected on other NRs including glucocorticoid receptor, progesterone receptor, vitamin D receptor (VDR), retinoic acid receptor and peroxisome proliferator activated receptor-γ (PPAR-γ) (data not shown).

Because ERs possess two transactivation functions, AF-1 and AF-2, in the amino-terminal A/B and carboxy-terminal E/F regions, respectively[16,20], we examined the functional association of AhR/Arnt with these two regions using ER deletion mutants (HE15 for AF-1 domain, and HE19 for AF-2 domain) (Supplementary Fig. 1b) in Ishikawa cells. The N-terminal A/B regions of ER-α and ER-β were required for stimulation of ERE-mediated transcription by AhR/Arnt, whereas we detected no modulation of AF-2 functions (Fig. 1e)[20]. Thus, 3MC-bound AhR/Arnt might modulate the functions of ERs through association with the N-terminal A/B regions. This possibility was supported by the observation that

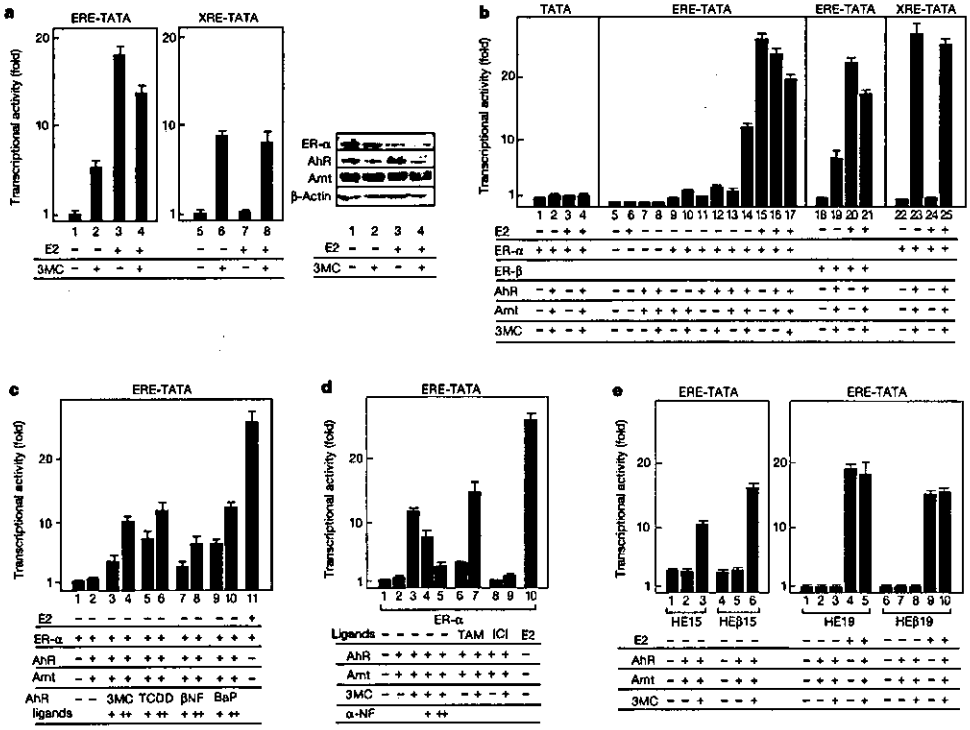

Figure 1 Activation of unliganded ER function by liganded dioxin receptor heterodimer. **a**, A dioxin receptor ligand activates transcription mediated through an ERE. MCF-7 cells were transfected with the reporter plasmids ERE-luciferase or XRE-luciferase in the presence or absence of E2 (10 nM) and 3MC (1 μM). Luciferase assays were performed with the cell extracts. All values are means ± s.d. for at least three independent experiments. **b**, Liganded AhR/Arnt induces the transactivation function of ERE-bound unliganded ER. Ishikawa cells transfected with the indicated plasmids were subjected to luciferase assays. **c**, Transactivation of unliganded ER by the other AhR agonists. **d**, Potentiation of ERE-mediated transcription by liganded AhR/Arnt is blocked by an antagonist for either ER-α or AhR. Cells treated with tamoxifen (TAM; 100 nM), ICI182,780 (ICI; 100 nM), 3MC (+, 100 nM; ++, 1 μM), TCDD (+, 10 nM; ++, 100 nM), β-naphthoflavone (β-NF; +, 100 nM; ++, 1 μM), benzo[*a*]pyrene (BaP; +, 10 nM; ++, 100 nM), α-naphthoflavone (α-NF; +, 100 nM; ++, 1 μM). **e**, Potentiation of ERE-mediated transcription by AhR/Arnt is mediated by the ERs A/B regions.

3MC-bound AhR/Arnt potentiates the transactivation function of ER-α in the presence of the ER-α AF-1 agonist/AF-2 antagonist tamoxifen (Fig. 1d)[16].

We then tested whether a 3MC-dependent physical interaction occurred between AhR/Arnt and ERs. Irrespective of E2 binding, endogenous ER-α in MCF-7 cells, and tagged ER-α overexpressed in COS-1 cells, were found to co-immunoprecipitate with 3MC-bound AhR, but not with unliganded AhR, only when Arnt was co-expressed (Fig. 2a and b). In agreement with the functional interaction between AhR/Arnt and the A/B region of ER-α (Fig. 1e), a 3MC-dependent interaction between AhR/Arnt and HE15 was observed, but not between AhR/Arnt and HE19 (ref. 12). Although ER-β, like ER-α, also associated with AhR in a 3MC-dependent fashion, no other receptors tested showed such an association (Fig. 2b).

Moreover, a direct interaction between AhR, but not Arnt, and A/B regions from both ER-α and ER-β could be mapped by an *in vitro* glutathione *S*-transferase (GST) pull-down assay (Fig. 2c). It therefore seems that, upon ligand binding and nuclear translocation[10], AhR heterodimerizes with nuclear Arnt and then associates with unliganded ER-α or ER-β, which are constitutively in the nucleus[16], through direct interaction with their A/B regions. Further analyses by GST pull-down assay mapped the small regions of the A/B region of ER-α (residues 40–120), the A/B region of ER-β (residues 33–55)[21], and the helix–loop–helix/PAS domain of AhR[22], which are indispensable for direct interaction *in vitro* (Fig. 2d and Supplementary Fig. 2a). An ER-α mutant lacking the AhR-interacting region (ER-α ΔAhR) failed to be activated by AhR/Arnt but responsiveness to E2 was still retained, supporting the idea that the interaction is required for AhR ligand-induced activation of the ER function (Fig. 2e).

To explore the molecular mechanisms of the 3MC-dependent transactivation function of AhR and ERs, we used co-immunoprecipitation to examine whether p300 was recruited to the complex, because both AhR and ERs have been independently reported to require p300/CRB as a co-activator[10,16,18,23]. p300 was recruited to ER-α in the presence but not the absence of E2 (Fig. 2f, lanes 2 and 4). However, even in the absence of E2, p300 associated with 3MC-bound AhR/Arnt and unliganded ER-α to form a complex (Fig. 2f, lane 3). Recruitment of the p160 family co-activator SRC-1 (ref. 13; Fig. 2f, lane 3), TIF2 or AIB1 (data not shown) to AhR/Arnt-associated ERs were not detected. Thus, the co-activator complex required to activate transcription by the unliganded ERs associated with liganded AhR/Arnt might be distinct from both co-activator

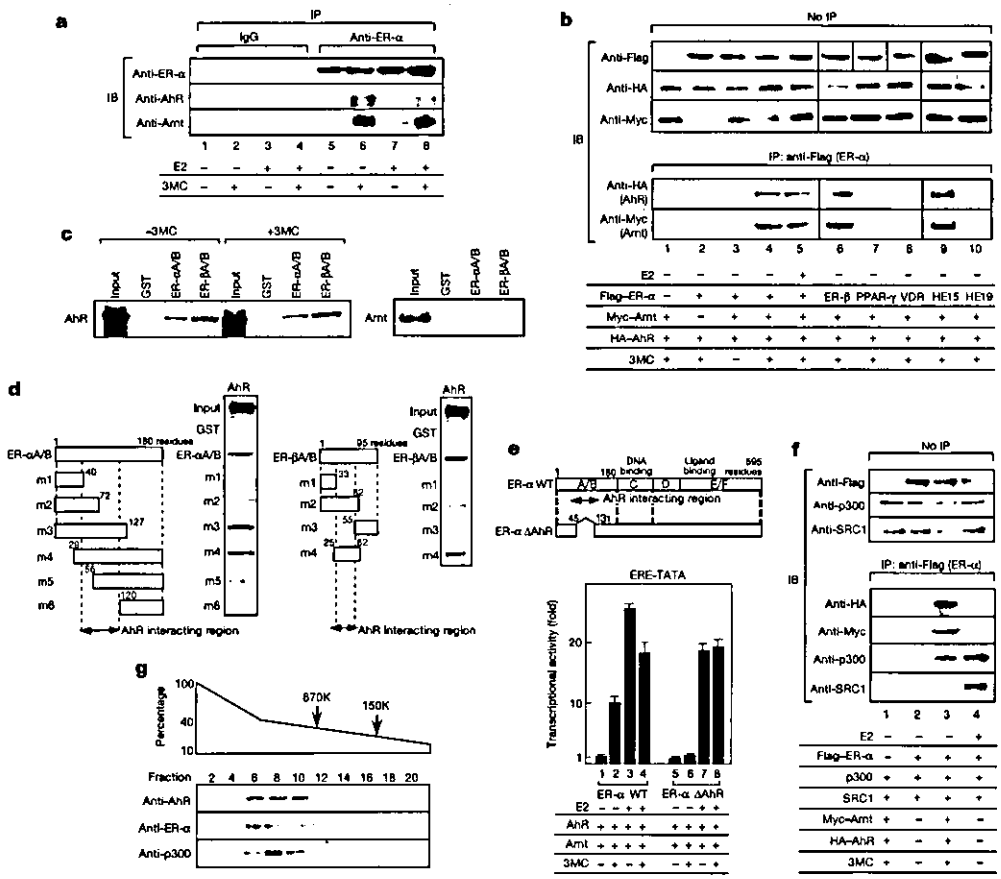

Figure 2 3MC-dependent interaction of ERs with AhR/Arnt. **a**, 3MC-dependent but E2-independent interaction of endogenous ER-α with AhR/Arnt in MCF-7 cells. Cells were subjected to immunoprecipitation (IP) with mouse anti-ER-α or normal mouse immunoglobulin as a control. The immunoprecipitates were western blotted (IB) with specific antibodies as indicated. **b**, E2-independent, 3MC-dependent interaction of exogenous ERs with AhR/Arnt in COS-1 cells. The transfected cells were subjected to immunoprecipitation and then western blotting. PPAR, peroxisomeproliferatoractivated receptor; VDR, vitamin D receptor. **c**, Direct but 3MC-independent interaction of AhR with ER-α and ER-β in an *in vitro* GST pull-down assay. **d**, Mapping the interaction domains of ER-α and ER-β with AhR. **e**, The AhR-interacting core region in the ER-α A/B domain is required for ER-α activation by AhR/Arnt. Luciferase assays with the indicated ER derivative. **f**, Recruitment of p300 co-activator to a complex containing unliganded ER-α and 3MC-bound AhR/Arnt. **g**, AhR/ER-α/p300 form a complex on glycerol gradient analysis. The Flag–AhR associated proteins in stable transformant HeLa cells were fractionated by molecular mass by a glycerol gradient assay.

complexes for the unassociated receptors. Indeed, ER-α and p300 were detected in the same fractions as Flag ($[EYKEEEK]_2$)-tagged AhR fractionated by a glycerol gradient, suggesting that they form a complex with a relative molecular mass (M_r) larger than 670,000 (670K) (Fig. 2g).

To investigate whether the observed association between AhR and ERs occurred on EREs in endogenous target gene promoters of MCF-7 cells, we performed a chromatin immunoprecipitation (ChIP) analysis with *pS2* and c-*fos* gene promoters[17]. Interestingly, 3MC induced binding of ER-α to ERE, as did E2, with AhR/Arnt recruitment. As expected, 3MC induced the recruitment of AhR/Arnt, but not ER-α, to the *CYP1A1* promoter XRE (Fig. 3a). Reflecting the recruitment of the receptors, acetylation of histone H4 was observed in the promoters (Fig. 3a), indicating the possible recruitment of a HAT co-activator complex to the receptors. The expression of these genes was accordingly induced by 3MC or E2 (Fig. 3d). Thus, the 3MC-dependent association between AhR/Arnt and ER-α seems to promote the binding of unliganded ER-α to EREs.

A ChIP assay involving sequential immunoprecipitation confirmed the 3MC-dependent association of AhR/Arnt with ER-α on

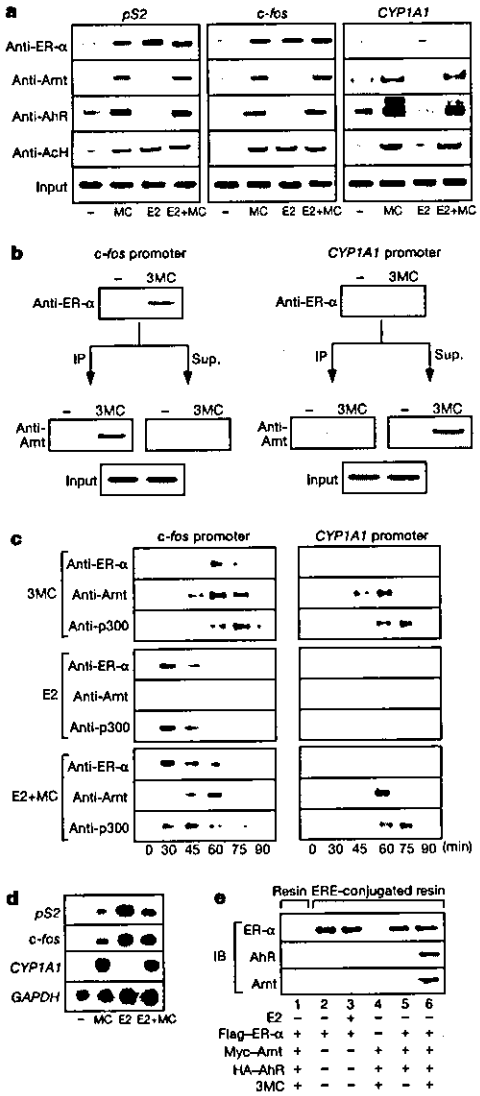

Figure 3 3MC-dependent recruitment of AhR/Arnt to ER-α bound on oestrogen-responsive gene promoters. **a**, 3MC-dependent interaction with AhR/Arnt induces ERE binding of unliganded ER-α to E2 responsive gene promoters in MCF-7 cells. For ChIP analyses, soluble chromatin prepared from MCF-7 cells treated with ligands for 45 min was immunoprecipitated with the indicated antibodies. The final DNA extracts were amplified using specific sets of primer pairs to detect the c-*fos*, *pS2* and *CYP1A1* gene promoters as indicated. **b**, 3MC-dependent association of AhR/Arnt with ER-α bound to E2-responsive gene promoters. The immunoprecipitates and their supernatants were sequentially applied for ChIP analysis as indicated. **c**, Dynamics of ER-α–Arnt–p300 assembly on ligand-responsive gene promoters. Occupancy of the c-*fos* and *CYP1A1* promoters by ER-α, Arnt and p300 at different times after ligand treatments. **d**, Induction of target genes examined by northern blot analysis. **e**, Complex formation of AhR–Arnt–ER-α on ERE through ER-α as revealed by ABCD assay.

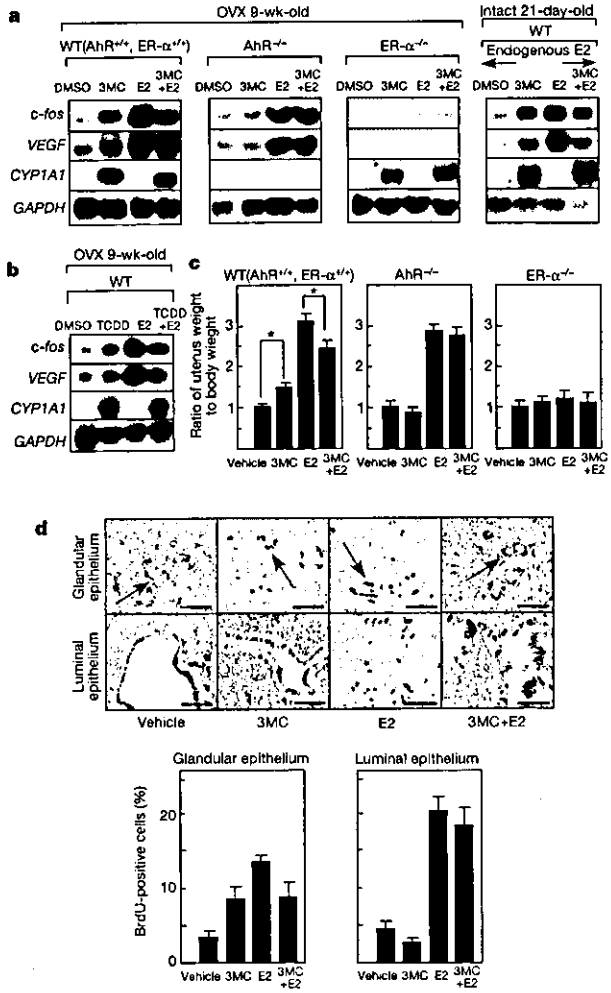

Figure 4 Oestrogenic actions of 3MC in mouse uterus are mediated by AhR and ER-α. **a**, **b**, Induction of E2-responsive genes by AhR agonists is mediated by both AhR and ER-α. Nine-week-old ovariectomized (OVX) mice and intact 21-day-old female mice of the indicated genotypes were injected with the ligands. Three hours later, total RNA was extracted from the uterus, then subjected to northern blot analysis with cDNAs for the target genes for E2 (c-*fos*, *VEGF*) and for 3MC (*CYP1A1*); *GAPDH* cDNA was used as an internal control. WT, wild type. **c**, The 3MC-induced increase in uterine wet weight (measured as the ratio of uterine wet weight in milligrams to body weight in grams) in ovariectomized mice was abolished by inactivation by either AhR or ER-α. The *t*-test shows a significant difference ($P < 0.01$) between 3MC-treated ($n = 9$) and olive-oil-treated ($n = 9$) wild-type mice. There is no significant difference ($P > 0.2$) between 3MC-treated ($n = 4$) and olive-oil-treated ($n = 4$) animals in either $AhR^{-/-}$ and $ER\text{-}\alpha^{-/-}$ mice. All values are means ± s.e.m. **d**, Induction of endometrial cell proliferation by 3MC and E2. BrdU-positive cells (brown) are indicated by arrows.

ERE (Fig. 3b). A time-course ChIP assay showed that ER-α, AhR and p300 HAT were simultaneously recruited to the c-*fos* promoter, presumably upon the binding of 3MC to AhR (Fig. 3c).

To verify the interaction of AhR/Arnt with ER-α bound to ERE in the promoters, the formation of a complex with ERE was tested by avidin–biotin-conjugated DNA(ERE) (ABCD) precipitation[24] (Fig. 3e). ER-α bound to consensus ERE (Fig. 3e, lanes 2, 3, 5 and 6), whereas AhR/Arnt alone did not (Fig. 3e, lane 4). However, in the presence of ER-α, AhR/Arnt was recruited to ERE in a 3MC-dependent manner (Fig. 3e, lanes 5 and 6). In the transient luciferase assay, the binding of ER-α to ERE and the activation function of both AhR and Arnt were required for the activation of ER-α through ERE by AhR/Arnt (Supplementary Fig. 3a, lanes 3, 7, and 8), whereas the AF-1 and AF-2 activities of ER-α and the DNA-binding capacity of the AhR/Arnt heterodimer were dispensable (Supplementary Fig. 3a, lanes 4–6).

Finally, we tested whether AhR-ligand-dependent AhR–ER interaction was responsible for the oestrogenic actions of AhR agonists in the absence of oestrogens on gene expression in intact animals. In addition to the induction of the *CYP1A1* gene, treatments with 3MC (Fig. 4a) and TCDD (Fig. 4b) for 3 hours stimulated the expression of the oestrogen-responsive genes c-*fos*[25] and *vascular endothelial growth factor* (*VEGF*)[26] in the uteri of ovariectomized wild-type mice (Fig. 4a, b). This oestrogenic action of 3MC in the uterus was also detected in intact 21-day-old female mice, whereas the AhR agonists exhibited anti-oestrogenic activities in the presence of high doses of oestrogen (Fig. 4a). There have been conflicting reports on the induction of c-*fos* by AhR ligands: one is that AhR ligands repress the E2-induced expression of c-*fos*[3]; the other is that AhR ligands themselves induce the expression of c-*fos*[27]. The 3MC-mediated activation of oestrogen target genes was completely abolished in both $AhR^{-/-}$ (ref. 28) and ER-$\alpha^{-/-}$ (ref. 29) ovariectomized mice, although each receptor knockout mouse strain retained ligand responsiveness (Fig. 4a) and the expression (Supplementary Fig. 4a) of the other intact receptor. The injection of 3MC led to increases in uterine wet weight, as did that of E2 (Fig. 4c). This action of 3MC was again abolished in both $AhR^{-/-}$ and ER-$\alpha^{-/-}$ mice (Fig. 4c).

To examine whether the increased uterine wet weight was due to the proliferation of endometrial cells, DNA synthesis in uterine epithelial cells was examined by labelling with bromodeoxyuridine (BrdU). Ovariectomized mice treated with 3MC exhibited enhanced cell proliferation in the glandular epithelium, as did E2-treated mice (Fig. 4d). Proliferation of the luminal epithelium was enhanced by E2 but not by 3MC.

The present findings indicate that the oestrogenic action of AhR agonists might be exerted through a direct interaction between AhR/Arnt and unliganded ER and by the formation of functional units bound to EREs that activate transcription, at least in uterine gene induction and cellular proliferation. The most marked manifestation of the possible oestrogenicity of dioxins could be seen as their linking to endometriosis[4–7], because oestrogen is the major factor in the stimulation of proliferation of these cells. Thus, AhR expressed in the uterine glandular epithelium[30] might respond to dioxins by associating with unliganded ERs, which then stimulates oestrogen-dependent cell proliferation. In contrast, AhR agonists exhibit anti-oestrogenic activities in the presence of high doses of E2 in animals[3] and cultured cell lines[2]. We also found that AhR/Arnt repressed E2-bound ER function, which is consistent with these previous reports. However, whereas most previous studies have not examined or mentioned the effects of AhR ligands in the absence of E2, we addressed this issue carefully in the present study. Thus, oestrogen concentrations, which vary with age, oestrous cycle, tissues and other factors, might define the oestrogenic/anti-oestrogenic actions of the AhR ligands in intact animals. Our present model, in which AhR potentiates unliganded ERs but represses liganded ER, might be an explanation of these previous findings, and it will be of interest to identify the other components of the liganded AhR–ER-α complex involved in the oestrogenic/anti-oestrogenic actions of dioxins. Our proposal is that one of the molecular mechanisms for the oestrogen-related adverse effects of dioxin-type environmental contaminants is the modulation of oestrogen receptor signalling by dioxin-dependent association with dioxin receptor. □

Methods

Plasmids

Full-length complementary DNAs of AhR and Arnt were inserted into pcDNA3 vectors (Invitrogen). Three consensus EREs[19] and XREs[22] were inserted into the promoter of luciferase pGL3-basic vector to generate ERE-TATA–luciferase and XRE-TATA–luciferase, respectively. ER-α ΔAhR was generated by the deletion of 45–131 residues from ER-α. The other mutants of ER-α and ER-β were as described previously[21].

Transfection and luciferase assay

Human endometrium cancer-derived Ishikawa cells, human breast cancer-derived MCF-7 cells, green monkey COS-1 cells and human 293T cells maintained in DMEM supplemented with 10% FBS were cultured in phenol-red-free DMEM containing 0.2% charcoal-stripped FBS before assays. Cells at 40–50% confluence were transfected with the indicated plasmids (0.25 μg ERE-Luc, 0.1 μg XRE-Luc, 0.025 μg ER-α, AhR and Arnt were transfected) using Lipofectamine reagent (Gibco BRL) in 12-well Petri dishes. Total amounts of cDNA were adjusted by supplementing with empty vector up to 1.0 μg. Cells were treated with E2 (100 nM) and 3MC (1 μM). Luciferase activity was determined with the Luciferase Assay System (Promega)[18]. As a reference plasmid to normalize transfection efficiency, 25 ng pRL-CMV plasmid (Promega) was co-transfected in all experiments. Results are given as means ± s.d. for at least three independent experiments.

Immunoprecipitation and GST pull-down assay

Whole cell extracts[17] were used for immunoprecipitation with either anti-ER-α or anti-Flag antibody (anti-ER-α Ab-4 from Neo Markers; anti-Flag from Santa Cruz Biotechnology) after western blotting with anti-ER-α (Chemicon), anti-Arnt (Santa Cruz Biotechnology), anti-AhR (Santa Cruz Biotechnology), anti-p300 (Upstate Biotechnology), anti-SRC-1 (Santa Cruz Biotechnology), anti-Flag, anti-haemagglutinin and anti-Myc (Invitrogen) antibodies. Normal mouse immunoglobulin was used as a control. For immunoprecipitation of overexpressed proteins, cells were transfected as indicated with Flag-tagged ERs (5 μg), haemagglutinin-tagged AhR (3 μg), Myc-Arnt (5 μg), SRC-1 (0.7 μg) and p300 (0.7 μg) in the presence or absence of 3MC and E2. For the GST pull-down assay, AhR and Arnt were translated *in vitro* and incubated with either GST, GST–ER-α(A/B) or GST–ER-β(A/B) immobilized on glutathione–Sepharose beads[17].

Purification and separation of AhR-interacting complexes

HeLa nuclear extracts were loaded on an M2 anti-Flag agarose gel (Kodak). After being washed with binding buffer, the bound proteins were eluted from the agarose by incubation overnight with 2.5–5.0 ml of the Flag peptide (Kodak) in binding buffer (0.2 mg ml^{-1}). For fractionation on a glycerol gradient, eluents were layered on the top of a 13-ml linear 100–10% glycerol gradient and centrifuged for 16 h at 40,000 r.p.m. in an SW40 rotor (Beckman). Each fraction was western blotted with anti-AhR, anti-ER-α and anti-p300 antibodies. The protein standards used were β-globulin (*M*, 158K) and thyroglobulin (667K)[17].

Chromatin immunoprecipitation

Soluble chromatins of MCF-7 cells prepared with the acetyl-histone H4 immunoprecipitation assay kit (Upstate Biotechnology) were immunoprecipitated with antibodies against the indicated proteins. Specific primer pairs were designated to amplify the promoter regions of the c-*fos* (5′-GAAGAGTGGAGAAGGG-3′ and 5′-GAAGCTGTGCTTACGG-3′), *pS2* (5′-AAAGAATTAGCTTAGGCC-3′ and 5′-ACCTTAATCCAGGTCC-3′) or *CYP1A1* (5′-CTTCGCCATCCATTCC-3′ and 5′-GGGACTCCTCTTCGAC-3′) genes from the extracted DNA. Optimal PCR conditions to allow semiquantitative measurement were used on 2% agarose/Tris-acetate-EDTA gels[17]. As a usual condition, cells were treated with ligands for 45 min. The inductions of the target genes were examined by northern blot analysis in MCF-7 cells treated with the ligands for 3 h.

ABCD precipitation

Avidin resin (Promega) was incubated with biotin-conjugated consensus ERE oligonucleotides, followed by incubation with cell lysates in lysis buffer (20 mM HEPES, 100 mM KCl, 0.5 mM EDTA, 0.1% Triton X-100 and 1 mM dithiothreitol) for 30 min. The subsequent ERE–protein complexes trapped on the resin were then eluted and western blotted[24].

Oestrogen responses in uterus

Nine-week-old female C57BL/6 mice with the indicated genotypes were ovariectomized. After 2 weeks the mice were treated with 3MC (4 mg kg^{-1}), TCDD (40 μg kg^{-1}), and/or E2 (20 μg kg^{-1}) in olive oil for 3 h. Total RNA was extracted from the uteri by Isogen (Wako Co.) and then subjected to northern blot analysis with cDNAs for the target genes for E2 (c-*fos*, *VEGF*) and for 3MC (*CYP1A1*), with *GAPDH* cDNA (encoding glyceraldehydes-3-

phosphate dehydrogenase) as an internal control[16]. For experiments with intact mice, 21-day-old female mice were used.

For uterine weight analysis, mice were treated with ligands for 3 days, and the ratio of uterine wet weight to body weight was calculated, followed by *t*-test analysis. Results are given as means ± s.e.m.

For the BrdU labelling experiment, ovariectomized mice were treated with ligands for 3 days, then injected with BrdU (30 mg kg^{-1}). Paraffin sections from the uteri 8 h after BrdU injection were immunostained with anti-BrdU monoclonal antibody by using the BrdU Labeling and Detection Kit I (Roche), and the percentage of BrdU-positive epithelial cells in the sections was calculated.

Received 19 February; accepted 1 April 2003; doi:10.1038/nature01606.

1. Bock, K. W. Aryl hydrocarbon or dioxin receptor: biologic and toxic responses. *Rev. Physiol. Biochem. Pharmacol.* **125,** 1–42 (1994).
2. Krishnan, V. *et al.* Molecular mechanism of inhibition of estrogen-induced cathepsin D gene expression by 2,3,7,8-tetrachlorodibenzo-*p*-dioxin (TCDD) in MCF-7 cells. *Mol. Cell. Biol.* **15,** 6710–6719 (1995).
3. Astroff, B. *et al.* Inhibition of the 17β-estradiol-induced and constitutive expression of the cellular protooncogene *c-fos* by 2,3,7,8-tetrachlorodibenzo-*p*-dioxin (TCDD) in the female rat uterus. *Toxicol. Lett.* **56,** 305–315 (1991).
4. Gibbons, A. Dioxin tied to endometriosis. *Science* **262,** 1373 (1993).
5. Mayani, A., Barel, S., Soback, S. & Almagor, M. Dioxin concentrations in women with endometriosis. *Hum. Reprod.* **12,** 373–375 (1997).
6. Rier, S. E., Martin, D. C., Bowman, R. E., Dmowski, W. P. & Becker, J. L. Endometriosis in rhesus monkeys (*Macaca mulatta*) following chronic exposure to 2,3,7,8-tetrachlorodibenzo-*p*-dioxin. *Fundam. Appl. Toxicol.* **21,** 433–441 (1993).
7. Cummings, A. M., Metcalf, J. L. & Birnbaum, L. Promotion of endometriosis by 2,3,7,8-tetrachlorodibenzo-*p*-dioxin in rats and mice: time–dose dependence and species comparison. *Toxicol. Appl. Pharmacol.* **138,** 131–139 (1996).
8. Brown, N. M., Manzolillo, P. A., Zhang, J. X., Wang, J. & Lamartiniere, C. A. Prenatal TCDD and predisposition to mammary cancer in the rat. *Carcinogenesis* **19,** 1623–1629 (1998).
9. Davis, B. J., McCurdy, E. A., Miller, B. D., Lucier, G. W. & Tritscher, A. M. Ovarian tumors in rats induced by chronic 2,3,7,8-tetrachlorodibenzo-*p*-dioxin treatment. *Cancer Res.* **60,** 5414–5419 (2000).
10. Sogawa, K. & Fujii-Kuriyama, Y. Ah receptor, a novel ligand-activated transcription factor. *J. Biochem. (Tokyo)* **122,** 1075–1079 (1997).
11. Schmidt, J. V. & Bradfield, C. A. Ah receptor signaling pathways. *Annu. Rev. Cell Dev. Biol.* **12,** 55–89 (1996).
12. Kato, S. *et al.* Activation of the estrogen receptor through phosphorylation by mitogen-activated protein kinase. *Science* **270,** 1491–1494 (1995).
13. McKenna, N. J. & O'Malley, B. W. Combinatorial control of gene expression by nuclear receptors and coregulators. *Cell* **108,** 465–474 (2002).
14. Mangelsdorf, D. J. *et al.* The nuclear receptor superfamily: the second decade. *Cell* **83,** 835–839 (1995).
15. Freedman, L. P. Increasing the complexity of coactivation in nuclear receptor signaling. *Cell* **97,** 5–8 (1999).
16. Watanabe, M. *et al.* A subfamily of RNA-binding DEAD-box proteins acts as an estrogen receptor alpha coactivator through the N-terminal activation domain (AF-1) with an RNA coactivator, SRA. *EMBO J.* **20,** 1341–1352 (2001).
17. Yanagisawa, J. *et al.* Nuclear receptor function requires a TFTC-type histone acetyl transferase complex. *Mol. Cell* **9,** 553–562 (2002).
18. Kamei, Y. *et al.* A CBP integrator complex mediates transcriptional activation and AP-1 inhibition by nuclear receptors. *Cell* **85,** 403–414 (1996).
19. Tian, Y., Ke, S., Thomas, T., Meeker, R. J. & Gallo, M. A. Transcriptional suppression of estrogen receptor gene expression by 2,3,7,8-tetrachlorodibenzo-*p*-dioxin (TCDD). *J. Steroid Biochem. Mol. Biol.* **67,** 17–24 (1998).
20. Tora, L. *et al.* The human estrogen receptor has two independent nonacidic transcriptional activation functions. *Cell* **59,** 477–487 (1989).
21. Kobayashi, Y. *et al.* p300 mediates functional synergism between AP-1 and AF-2 of estrogen receptor alpha and beta by interacting directly with the N-terminal A/B domains. *J. Biol. Chem.* **275,** 15645–15651 (2000).
22. Mimura, J., Ema, M., Sogawa, K. & Fujii-Kuriyama, Y. Identification of a novel mechanism of regulation of Ah (dioxin) receptor function. *Genes Dev.* **13,** 20–25 (1999).
23. Beischlag, T. V. *et al.* Recruitment of the NCoA/SRC-1/p160 family of transcriptional coactivators by the aryl hydrocarbon receptor/aryl hydrocarbon receptor nuclear translocator complex. *Mol. Cell. Biol.* **22,** 4319–4333 (2002).
24. Daitoku, H. Y. K., Matsuzaki, H., Hatta, M. & Fukamizu, A. Regulation of PGC-1 promoter activity by protein kinase B and the forkhead transcription factor FKHR. *Diabetes* **52,** 642–649 (2003).
25. Weisz, A. & Rossles, R. Identification of an estrogen response element upstream of the human *c-fos* gene that binds the estrogen receptor and the AP-1 transcription factor. *Nucleic Acids Res.* **18,** 5097–5106 (1990).
26. Mueller, M. D. *et al.* Regulation of vascular endothelial growth factor (VEGF) gene transcription by estrogen receptors alpha and beta. *Proc. Natl Acad. Sci. USA* **97,** 10972–10977 (2000).
27. Puga, A., Nebert, D. W. & Carrier, F. Dioxin induces expression of *c-fos* and *c-jun* proto-oncogenes and a large increase in transcription factor AP-1. *DNA Cell Biol.* **11,** 269–281 (1992).
28. Mimura, J. *et al.* Loss of teratogenic response to 2,3,7,8-tetrachlorodibenzo-*p*-dioxin (TCDD) in mice lacking the Ah (dioxin) receptor. *Genes Cells* **2,** 645–654 (1997).
29. Dupont, S. *et al.* Effect of single and compound knockouts of estrogen receptors α (ERα) and β (ERβ) on mouse reproductive phenotypes. *Development* **127,** 4277–4291 (2000).
30. Kuchenhoff, A. *et al.* Arylhydrocarbon receptor expression in the human endometrium. *Fertil. Steril.* **71,** 354–360 (1999).

Supplementary Information accompanies the paper on **www.nature.com/nature.**

Acknowledgements We thank K. Korach and A. Fukamizu for helpful discussion; T. Sato, A. Murayama and Y. Kobayashi for technical assistance; Taiho Pharmaceutical Co. for ER ligands; and R. Nakamura and H. Higuchi for manuscript preparation. This work was supported in part by grants-in-aid for priority areas from the Ministry of Education, Science, Sports and Culture of Japan (to Y.F.-K. and S.K.).

Competing interests statement The authors declare that they have no competing financial interests.

Correspondence and request s for materials should be addressed to S.K. (uskato@mail.ecc.u-tokyo.ac.jp).

Insulin-regulated hepatic gluconeogenesis through FOXO1–PGC-1α interaction

Pere Puigserver*†, James Rhee*, Jerry Donovan*, Christopher J. Walkey*, J. Cliff Yoon*, Francesco Oriente‡, Yukari Kitamura‡, Jennifer Altomonte§, Hongjiang Dong§, Domenico Accili‡ & Bruce M. Spiegelman*

** Dana-Farber Cancer Institute and Department of Cell Biology, Harvard Medical School, Boston, Massachusetts 02115, USA*
‡ Naomi Berrie Diabetes Center and Department of Medicine, College of Physicians & Surgeons of Columbia University, New York, New York 10032, USA
§ Institute for Human Gene Therapy and Molecular Medicine, Mount Sinai School of Medicine, New York, New York 10029, USA

Hepatic gluconeogenesis is absolutely required for survival during prolonged fasting or starvation, but is inappropriately activated in diabetes mellitus. Glucocorticoids and glucagon have strong gluconeogenic actions on the liver. In contrast, insulin suppresses hepatic gluconeogenesis[1–3]. Two components known to have important physiological roles in this process are the forkhead transcription factor FOXO1 (also known as FKHR) and peroxisome proliferative activated receptor-γ co-activator 1 (PGC-1α; also known as PPARGC1), a transcriptional co-activator; whether and how these factors collaborate has not been clear. Using wild-type and mutant alleles of FOXO1, here we show that PGC-1α binds and co-activates FOXO1 in a manner inhibited by Akt-mediated phosphorylation. Furthermore, FOXO1 function is required for the robust activation of gluconeogenic gene expression in hepatic cells and in mouse liver by PGC-1α. Insulin suppresses gluconeogenesis stimulated by PGC-1α but co-expression of a mutant allele of FOXO1 insensitive to insulin completely reverses this suppression in hepatocytes or transgenic mice. We conclude that FOXO1 and PGC-1α interact in the execution of a programme of powerful, insulin-regulated gluconeogenesis.

Two transcriptional components that are targets of insulin signalling, and that can activate the process of gluconeogenesis in liver, are FOXO1 and PGC-1α. FOXO1 has been shown to bind directly to the promoters of gluconeogenic genes and activate the process of glucose production[4–6]. FOXO1 is directly phosphorylated by Akt, a key protein kinase downstream of the insulin receptor[7,8]. This phosphorylation results in exclusion of FOXO1 from the nucleus. A second transcriptional component controlled by insulin and having a role in gluconeogenesis is the co-activator PGC-1α. PGC-1α is induced in liver on fasting, and is elevated in several models of diabetes or deficiency in insulin signalling. Notably, expression of PGC-1α at physiological levels turns on the entire programme of gluconeogenesis[9,10].

† Present address: Department of Cell Biology, Johns Hopkins University School of Medicine, Baltimore, Maryland 21205, USA

Cytokines suppress adipogenesis and PPAR-γ function through the TAK1/TAB1/NIK cascade

Miyuki Suzawa*, Ichiro Takada*, Junn Yanagisawa*, Fumiaki Ohtake*, Satoko Ogawa*‡, Toshimasa Yamauchi§, Takashi Kadowaki§, Yasuhiro Takeuchi¶, Hiroshi Shibuya‡, Yukiko Gotoh*, Kunihiro Matsumoto# and Shigeaki Kato*†**

*Institute of Molecular and Cellular Biosciences, University of Tokyo, Yayoi, Bunkyo-ku, Tokyo 113-0032, Japan
†CREST, Japan Science and Technology, 4-1-8 Honcho, Kawaguchi, Saitama 332-0012, Japan
‡Division of Morphogenesis, Department of Developmental Biology, National Institute for Basic Biology, Okazaki 444-8585, Japan
§Department of Metabolic Diseases, Graduate School of Medicine, University of Tokyo, Tokyo 113-8655, Japan
¶Division of Endocrinology Department of Medicine University of Tokyo School of Medicine, Mejirodai, Bunkyo-ku, Tokyo 112-8688, Japan
#Department of Molecular Biology, Graduate School of Science, Nagoya University, Chikusa-ku, Nagoya 464-8602, Japan
**e-mail: uskato@mail.ecc.u-tokyo.ac.jp

Published online: 24 February 2003; DOI: 10.1038/ncb942

Pluripotent mesenchymal stem cells in bone marrow differentiate into adipocytes, osteoblasts and other cells[1,2]. Balanced cytodifferentiation of stem cells is essential for the formation and maintenance of bone marrow; however, the mechanisms that control this balance remain largely unknown. Whereas cytokines such as interleukin-1 (IL-1) and tumour-necrosis factor-α (TNF-α) inhibit adipogenesis[3,4], the ligand-induced transcription factor peroxisome proliferator-activated receptor-γ[5] (PPAR-γ), is a key inducer of adipogenesis. Therefore, regulatory coupling between cytokine- and PPAR-γ-mediated signals might occur during adipogenesis. Here we show that the ligand-induced transactivation function of PPAR-γ is suppressed by IL-1 and TNF-α, and that this suppression is mediated through NF-κB activated by the TAK1/TAB1/NF-κB-inducing kinase (NIK) cascade[6–9], a downstream cascade associated with IL-1 and TNF-α signalling. Unlike suppression of the PPAR-γ transactivation function by mitogen-activated protein kinase-induced growth factor signalling through phosphorylation of the A/B domain[10], NF-κB blocks PPAR-γ binding to DNA by forming a complex with PPAR-γ and its AF-1-specific co-activator PGC-2. Our results suggest that expression of IL-1 and TNF-α in bone marrow may alter the fate of pluripotent mesenchymal stem cells, directing cellular differentiation towards osteoblasts rather than adipocytes by suppressing PPAR-γ function through NF-κB activated by the TAK1/TAB1/NIK cascade.

The cytokines IL-1 and TNF-α suppress adipogenesis in bone marrow pluripotent mesenchymal stem cells *in vivo* and *in vitro*[3,4]. By contrast, PPAR-γ functions as a key inducer of adipogenesis[5]. Consistent with these reports[3,4,10], we found that adipogenesis in ST2 cells, a mesenchymal cell line derived from mouse bone marrow, could be induced, as assessed by the observation of lipid-accumulating cells and the expression of adipocyte-associated differentiation markers such as AP2 and lipoprotein lipase (LPL), by treatment with low concentrations of the PPAR-γ ligand troglitazone and that this adipogenesis could be prevented by IL-1 or TNF-α (Fig. 1a, d). Consequently, ST2 cells treated with both troglitazone and cytokines differentiated into osteoblasts expressing both alkaline phosphatase (a marker of differentiation), a protein (Fig. 1b) and mRNA (Fig. 1d)[11].

This suppressive activity of cytokines was also observed when adipogenesis was weakly induced by the synthetic glucocorticoid dexamethasone (Fig. 1a). Troglitazone induced adipogenesis in primary cultured bone marrow cells of wild-type mice, and dexamethasone induced adipogenesis less strongly; however, the potency of both ligands was considerably reduced in PPAR-γ$^{+/-}$ cells[5] (Fig. 1c), suggesting that PPAR-γ is crucial for adipogenesis in bone marrow stem cells. The inhibitory action of TNF-α in troglitazone-induced adipogenesis was abolished in primary cultured bone marrow cells from mice lacking both TNF receptors I and II (TNF-RI$^{-/-}$II$^{-/-}$; ref. 12 and Fig. 1c).

The inhibitory effects of cytokines on adipogenesis in both ST2 and primary cultured cells (Fig. 1a, c) suggested that the ligand-induced transactivation function of the PPAR-γ might be suppressed by these cytokines. To investigate this, we first examined whether cytokine treatment over short time periods (12 h) caused a reduction in both the expression and the transactivation function of PPAR-γ using a transient expression assay with PPAR-γ and retinoid-X receptor-α (RXR-α) expression vectors and a luciferase reporter plasmid containing a consensus binding site (PPAR-response element; PPRE) for the PPAR-γ/RXR-α heterodimer[13,14]. The transactivation function of troglitazone-bound PPAR-γ was suppressed markedly in ST2 cells treated with either IL-1 or TNF-α, whereas the transactivation functions of dexamethasone-bound glucocorticoid receptor (GR) and C/EBP-β were not suppressed by either cytokine (Fig. 2a). The expression of both PPAR-γ and C/EBP-β seemed to be unchanged by cytokine treatment (Fig. 1d).

Because the cell membrane receptors for IL-1 and TNF-α can activate several downstream signalling cascades[6–9], we examined the activity of several mitogen-activated protein kinase (MAPK) cascades (MKK3, MKK6, MKK7, TAK1). Overexpression of TAK1 (refs 7–9), a MAPK kinase kinase (MAP3K), mimicked cytokine activity but only in the presence of TAB1, an activator of TAK1 (ref. 9 and Fig. 2b). By contrast, we did not detect suppressed PPAR-γ function in ST2 cells in the other MAPK cascades tested (MKK3, MKK6 and MKK7; Fig. 2c). Consistent with the observation that TAK1/TAB1 is a downstream factor of TNF-α and IL-1 signalling[6–8], a kinase-negative form of TAK1 (TAK1^{K63W}) abrogated

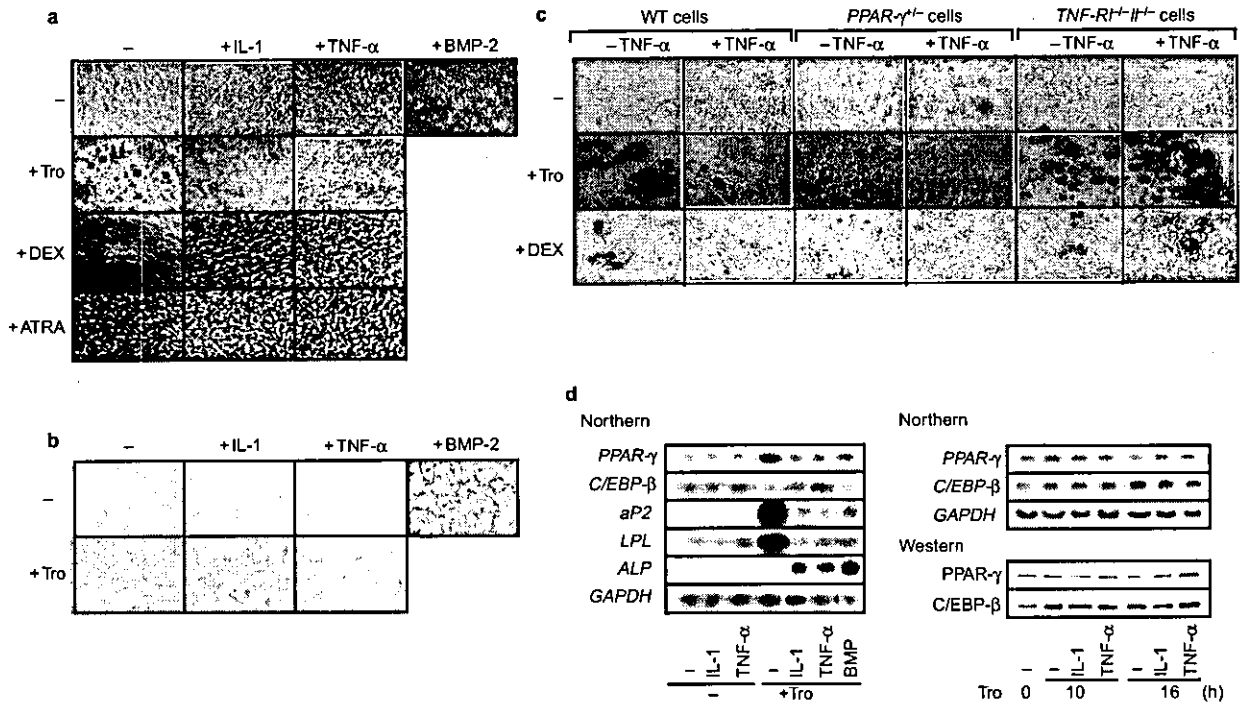

Figure 1 **IL-1 and TNF-α inhibit troglitazone-induced adipogenesis.** **a**, Inhibition of troglitazone- or dexamethasone-induced adipogenesis by IL-1 or TNF-α. Weak treatment (for 1 week) using the synthetic PPAR-γ ligand troglitazone (Tro) or dexamethasone (DEX), but not all-*trans* retinoic acid (ATRA), induces adipogenesis in ST2 cells. The presence of either IL-1 or TNF-α prevents this adipogenesis. Differentiated adipocytes were detected by the accumulation of lipid, which was stained red with Oil-Red-O. **b**, Combined treatment of cytokines and troglitazone induces osteoblastogenesis in ST2 cells. Cells were treated with cytokines and troglitazone as in **a**, and differentiated osteoblasts were stained by alkaline phosphatase. **c**, Adipocyte differentiation of wild-type, PPAR-γ$^{+/-}$ and TNF-RI$^{-/-}$II$^{-/-}$ mouse bone marrow. Primary cultured bone marrow cells derived from the corresponding mice were treated with troglitazone or dexamethasone with or without TNF-α. **d**, Differentiation of ST2 cells by troglitazone-expressed adipocyte-associated differentiation markers. Cells treated with cytokines and troglitazone for the indicated times were analysed both by northern blot for differentiation markers of adipocytes (aP2, LPL) and osteoblasts (ALP) and by western blot.

the suppressive effect of TAK1/TAB1, TNF-α and IL-1 on PPAR-γ transactivation.

We next examined NIK, a NF-κB-inducing kinase activated through phosphorylation by TAK1/TAB1 (which are activated in turn by TNF-α and IL-1)[7,8,15], for its ability to suppress PPAR-γ transactivation. Suppression mediated by NIK was clearly observed, but this suppression was abrogated when a dominant-negative form of NIK (NIK$^{629-947}$; ref. 7) was expressed (Fig. 2d). NIK$^{629-947}$ also abrogated the suppressive effects of TAK1/TAB1 and IL-1 or TNF-α treatment in ST2 cells (Fig. 2d). Consistent with these results, RNA-mediated interference (RNAi) of TAK1 and NIK expression effectively abrogated the suppressive effects of IL-1 or TNF-α in ST2 cells (Fig. 2e).

In accordance with the role of NIK in PPAR-γ transactivation, troglitazone-induced adipogenesis did not take place in stable transformants of the ST2 line expressing NIK (Fig. 2f), similar to what was observed in ST2 cells treated with TNF-α or IL-1 (Fig. 1a). By contrast, troglitazone-induced adipogenesis, even in the presence of cytokines, was observed after RNAi of TAK1 or NIK expression (Fig. 2h). As expected, adipogenesis in cell lines expressing the dominant-negative NIK$^{629-947}$ mutant was still troglitazone-sensitive; however, these NIK mutants failed to prevent the suppression of PPAR-γ transactivation through phosphorylation of Ser 112 in the A/B domain by a MAPK (ERK2) activated by the growth factor/Ras cascade (refs 10, 16 and Fig. 2g).

To determine whether the PPAR-γ transactivation function was suppressed by the TAK1/TAB1/NIK-mediated cascade or by the prevention of serine phosphorylation in the PPAR-γ A/B domain[10,16], we tested mutants in which each of the serines (Ser 8, Ser 118, Ser 274) was replaced with alanine, because analyses of the PPAR-γ deletion mutants suggested that the suppression of PPAR-γ function by cytokines was mediated by the AF-1 site in the A/B domain, and not by the AF-2 site in the carboxy terminus (data not shown). No difference in suppression was found between the wild-type and mutated receptors (Fig. 2g), suggesting that a distinct mechanism independent of serine phosphorylation in the PPAR-γ A/B domain is responsible for suppressing the PPAR-γ transactivation function. Highly similar effects of cytokines and NF-κB signal inducers on the PPAR-γ transactivation function were also seen using 293T cells, a human embryonic kidney cell line (data not shown).

To explore this molecular mechanism further, we examined the role of downstream factors of the TAK1/TAB1/NIK cascade. Overexpression of IKK-α and IKK-β, and treatment with H_2O_2 activated NF-κB[15], which then effectively suppressed the transactivation function of ligand-bound PPAR-γ in ST2 cells (Fig. 3a). In a co-immunoprecipitation assay with antibodies specific for PPAR-γ (refs 13 14), and for p50 or p65 from the NF-κB complex, we detected an association between endogenous NF-κB complex and endogenous troglitazone-bound PPAR-γ in ST2 cells, but only when cells were treated with either TNF-α or IL-1 (Fig. 3b), or when TAK1, TAB1 or NIK was overexpressed (data not shown).

Neither dexamethasone-bound GR (Fig. 3b) nor C/EBP-β (data not shown) showed this cytokine-induced association with NF-κB;

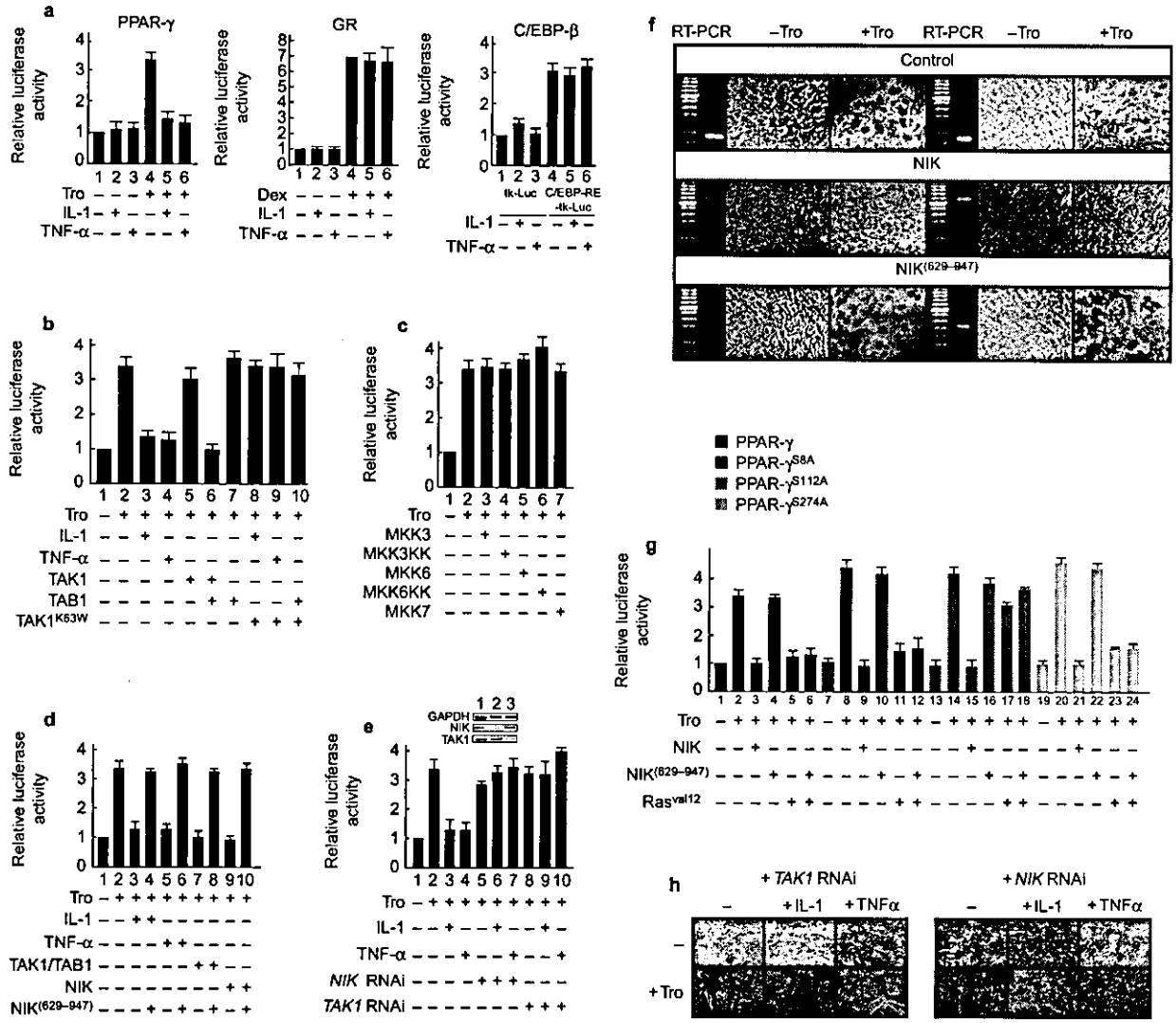

Figure 2 **TAK1/TAB1/NIK mediates suppression of PPAR-γ function.** **a**, The troglitazone-induced transactivation function of PPAR-γ is suppressed by IL-1 and TNF-α. ST2 cells were transfected with the indicated expression vectors plus mouse acyl-CoA–PPRE-tk, GRE-tk or C/EBP-RE-tk luciferase reporter plasmids and incubated for 16 h with the indicated cytokines in the absence or presence of cognate ligand. Similar results were obtained with 293T cell lines (not shown). **b**, Suppression of PPAR-γ transactivation function by TAK1/TAB1. ST2 cells were transfected with the indicated expression vectors plus the PPRE-tk luciferase reporter plasmid and incubated with the indicated cytokines for 16 h. **c**, Other MAP kinase cascades do not suppress PPAR-γ function. **d**, Suppression of PPAR-γ transactivation function by NIK. $NIK^{629-947}$ is a dominant-negative form of NIK. **e**, Suppression of PPAR-γ transactivation function by IL-1 or TNF-α is abrogated by RNAi of either NIK or TAK1. ST2 cells were co-transfected with the NIK or TAK1 RNAi vectors, and luciferase activity was assayed. Reduced expression of endogenous NIK and TAK1 was confirmed by RT–PCR (top). **f**, Inhibition of adipogenesis by NIK. ST2 stable transformants were established using the indicated NIK or $NIK^{529-947}$ expression vectors. Exogenous gene transcripts (control, 257 bp; NIK, 521 bp; $NIK^{529-947}$, 887 bp) were detected by RT–PCR. DNA molecular markers are shown in the left panels. Troglitazone-induced adipogenesis in stable transformants are shown in the right panels. **g**, The TAK1/TAB1 cascade potently inhibits phosphorylation-deficient mutants of PPAR-γ. The PPAR-γ mutants (S8A, S112A, S274A) were transfected along with NIK, $NIK^{629-947}$ or Ras^{val12} into ST2 cells. **h**, Inhibitory actions of cytokines are abolished by TAK1 or NIK RNAi. The RNAi vectors were transfected into ST2 cells and troglitazone-induced adipogenesis was examined.

thus, it seemed unlikely that the inhibited PPAR-γ transactivation function alone was responsible for the suppression of PPAR-γ function by NF-κB. We therefore tested the DNA-binding activity of endogenous PPAR-γ/RXR-α heterodimers by electrophoretic mobility shift assay (EMSA) using nuclear extracts from cytokine-treated cells. Both cytokine treatment (Fig. 3c) and overexpression of downstream factors and NF-κB (Fig. 3d) caused a considerable reduction in the ability of PPAR-γ/RXR-α heterodimers to bind to a consensus DNA-binding site (acyl-CoA-PPRE) in ST2 cells and 293T cells (data not shown), suggesting that PPAR-γ/RXR-α associates directly with NF-κB in cell nuclei. By contrast, cytokine treatment did not clearly inhibit DNA binding by GR in either cell line (data not shown).

We examined this association further with *in vitro* translated proteins and glutathione *S*-transferase (GST) fusion proteins (Fig. 3e, f). DNA binding by PPAR-γ/RXR-α was inhibited both by

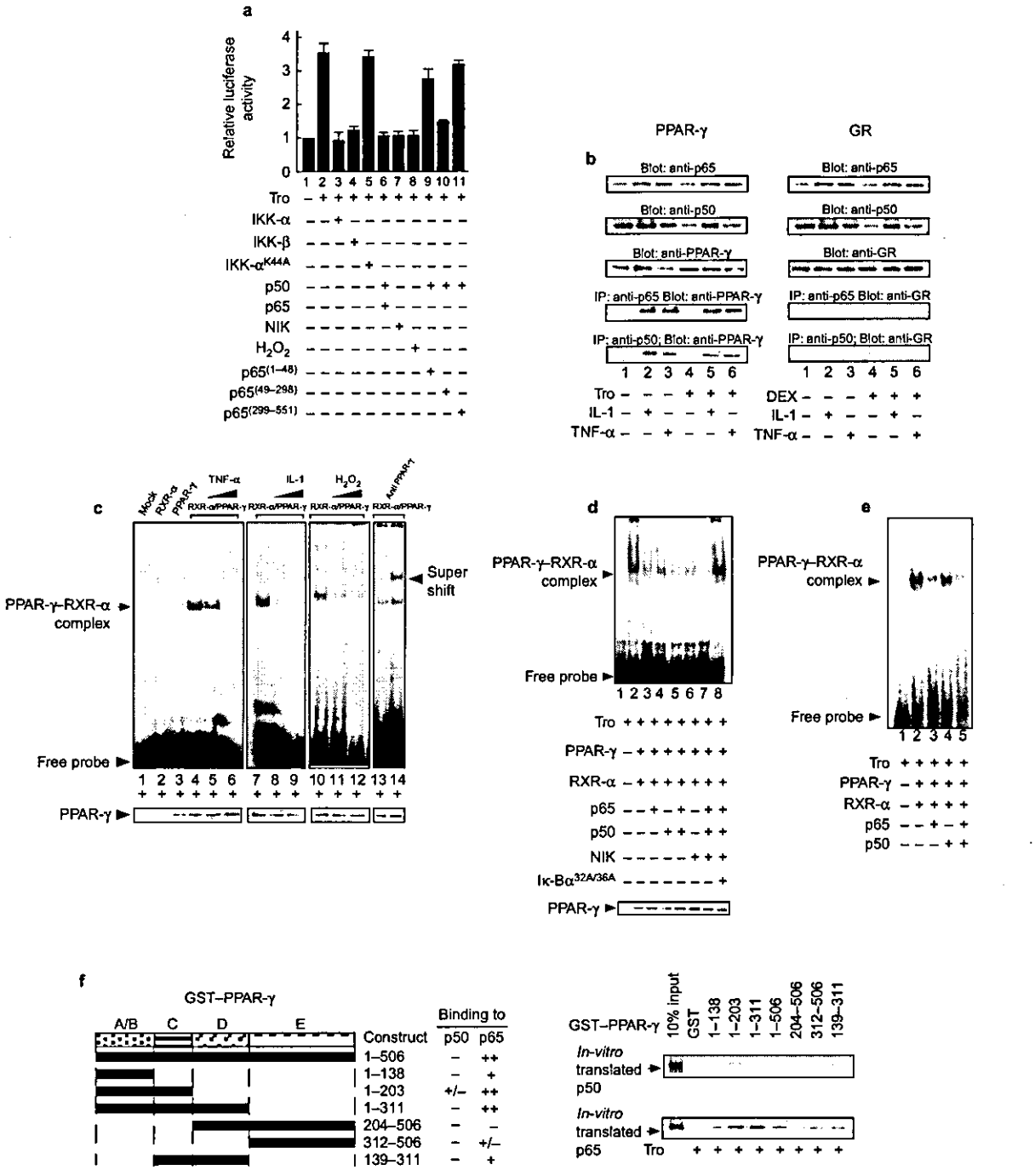

Figure 3 **NF-κB prevents DNA binding by the PPAR-γ/RXR-α heterodimer.** **a**, PPAR-γ function is suppressed by NIK-activated NF-κB. Vectors expressing the indicated signal inducers, which function downstream of NIK, were transfected into ST2 cell lines. **b**, NF-κB associates with PPAR-γ in the nucleus. Endogenous ligand-bound PPAR-γ and endogenous NF-κB complex were co-immunoprecipitated with antibodies against p65 or p50 (left) only when the cells were treated with cytokines. Cytokine treatment induced the association of PPAR-γ with the NF-κB complex in the nucleus. No endogenous GR was co-immunoprecipitated with the p65 or p50 antibodies (right). **c**, NF-κB-mediated inhibition of DNA binding by PPAR-γ is activated by cytokine signalling or H_2O_2 treatment. EMSA was done with nuclear extracts from ST2 cells transfected with the indicated expression vectors and treated with TNF-α (0.1 or 1 ng ml^{-1}), IL-1 (1.0 or 10 ng ml^{-1}) or H_2O_2 (0.1 or 1 mM). Expression of PPAR-γ was monitored by western blot using an antibody against PPAR-γ. A super-shift in the DNA-bound PPAR-γ/RXR-α heterodimer (lane 14) is indicated. **d**, Suppression of PPAR-γ DNA binding by NF-κB. IκBα$^{32A/36A}$ is a constitutive degradation-resistant mutant that inhibits NF-κB signalling[9]. **e**, Suppression of PPAR-γ DNA binding by NF-κB *in vitro*. *In vitro* translated p50, p65, PPAR-γ and RXR-α were used for EMSA as described in **c**. **f**, The NF-κB-interacting domain of PPAR-γ. GST fusion proteins of PPAR-γ deletion mutants were expressed in bacteria and used in GST pull-down assays with *in vitro* translated NF-κB.

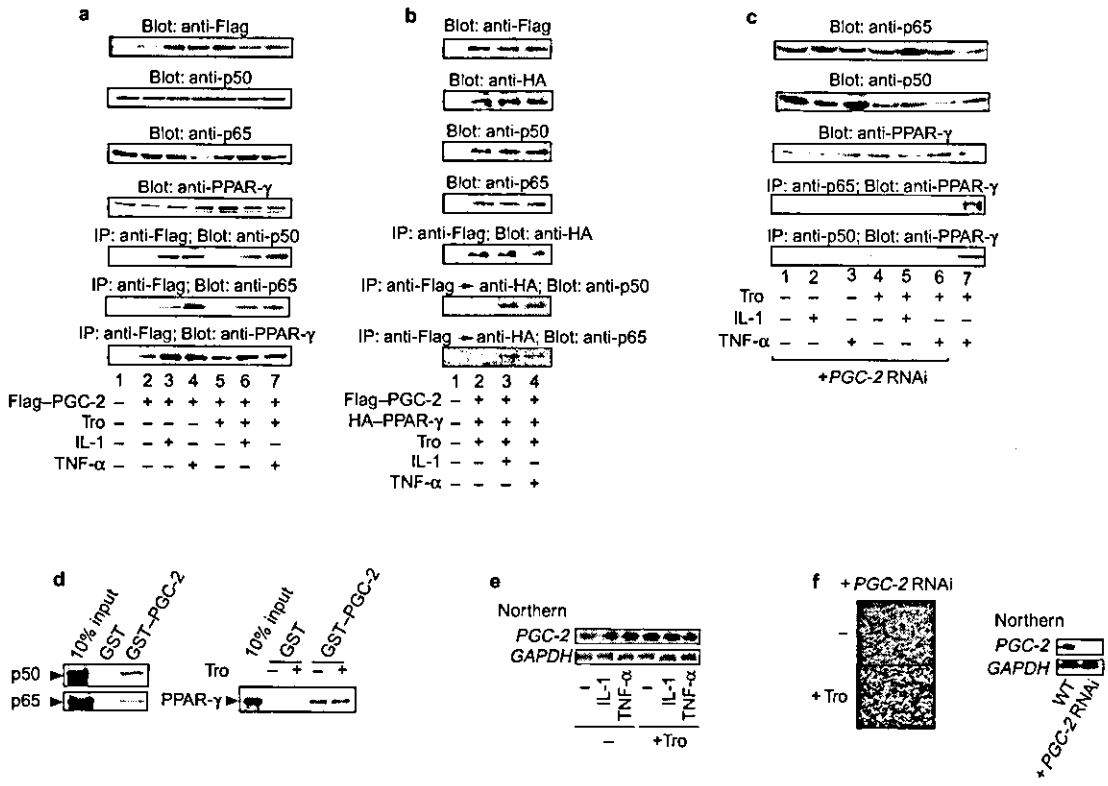

Figure 4 **Cytokine-induced association of PPAR-γ, NF-κB and PGC-2. a**, NF-κB associates with PGC-2. Exogenous Flag–PGC-2 and endogenous NF-κB complex were co-immunoprecipitated with antibodies against p65 or p50. **b**, Cytokine-dependent association of NF-κB with PGC-2 and PPAR-γ. ST2 cells transfected with Flag–PGC-2 and HA–PPAR-γ expression vectors were subjected to immunoprecipitation with antibodies against Flag, followed by antibodies against HA. NF-κB was co-immunoprecipitated with PGC-2 and PPAR-γ only when the cells were treated with cytokines. **c**, PGC-2 RNAi attenuates the cytokine-induced association of PPAR-γ/RXR with NF-κB. ST2 cells transfected with the PGC-2 RNAi vector were subjected to immunoprecipitation with antibodies against p65 or p50. **d**, PGC-2 interacts with NF-κB *in vitro*. Interaction of PGC-2 with either NF-κB (p50, p65) or PPAR-γ was examined by a GST pull-down assay. **e**, Cytokines and PPAR-γ ligand do not regulate PGC-2 expression in ST2 cells. Cells were treated with cytokines and troglitazone for 1 week and analysed by northern blot. **f**, PGC-2 RNAi attenuates troglitazone-induced adipogenesis in ST2 cells. Cells were transfected with PGC-2 RNAi vectors and treated with troglitazone to induce adipogenesis. Reduced expression of endogenous PGC-2 was confirmed by northern blot.

NF-κB and by p65 alone (Fig. 3e). The DNA-binding C domain of PPAR-γ was identified as a p65-interacting region (Fig. 3f), and a Rel-homology region (residues 49–298) in p65 (ref. 17) seemed to interact directly with PPAR-γ (data not shown) by GST pull-down assay. Accordingly, a $p65^{49-298}$ deletion mutant retained its function as an inhibitor of PPAR-γ (Fig. 3a), despite lacking the core DNA-binding domain[17].

We studied the molecular mechanism of the recruitment of NF-κB to PPAR-γ in bone marrow cell nuclei by examining potential PPAR-γ co-activators and co-repressors. Endogenous NF-κB did not associate directly with p160 family proteins (SRC-1/TIF2/AIB1)[13,14], DRIP205/TRAP220 (ref. 13) or NCoR/SMRT (data not shown), but it did associate directly with PGC-2, a PPAR-γ AF-1-specific co-activator (ref. 18 and Fig. 4a). This cytokine-induced interaction was detected when the complex was immunoprecipitated sequentially with PGC-2 and then PPAR-γ (Fig. 4b, c), suggesting that NF-κB associates with PGC-2-bound PPAR-γ. PGC-2 also interacted directly with NF-κB and PPAR-γ in the GST pull-down assay (Fig. 4d). Note that expression of the PGC-2 gene was unchanged by any treatment (Fig. 4e) and that the troglitazone-induced adipogenesis was attenuated by RNAi of PGC-2 expression (Fig. 4f). These findings suggest that NF-κB translocating into the nuclei is preferentially recruited to PPAR-γ through direct association with PGC-2, forming a complex that inhibits DNA binding by PPAR-γ.

We next tested whether the suppression of PPAR-γ function by the TAK1/TAB1/NIK cascade reflects physiological events in the transcriptional regulation of PPAR-γ target genes[5,19]. Induction of the early response gene encoding c-Cbl-associated protein (CAP) in response to the PPAR-γ ligand[19] was blocked by treatment with TNF-α or IL-1 (Fig. 5a). Consistent with these results, chromatin immunoprecipitation (ChIP) analysis[19,20] showed that troglitazone-induced histone (H4) acetylation around PPRE in the CAP gene promoter by PPAR-γ was abrogated by cytokine treatment (Fig. 5b). In addition, cytokine treatment blocked DNA binding by PPAR-γ, but not by GR and C/EBP-β (ref. 21 and Fig. 5b, bottom). Thus, these findings indicate that TNF-α and IL-1 signalling suppress the expression of endogenous target genes for PPAR-γ through NF-κB-mediated blocking of the binding of PPRE by endogenous PPAR-γ/RXR-α heterodimers, thereby exerting an inhibitory effect on adipogenesis.

Among the cytokines expressed in bone marrow, TNF-α and IL-1, which act as principal inducers of osteoclastogenesis from progenitor cells of monocyte/macrophage lineage[22], are known to inhibit adipogenesis[3,4], directing bone marrow stem cells towards osteoblastogenesis and the formation of trabecular bone[2]. But the molecular mechanisms by which these cytokines inhibit adipogenesis remain unclear. Given the wide acceptance of PPAR-γ as a principal inducer of adipogenesis[5], and the development of numerous

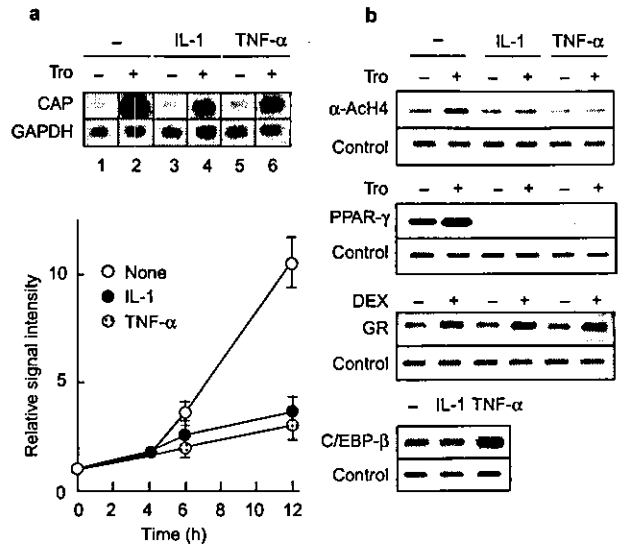

Figure 5 **Blocking PPAR-γ function inhibits adipogenesis through the NIK cascade. a**, Treatment with TNF-α or IL-1 prevents troglitazone-induced expression of an early response target gene of PPAR-γ. ST2 cells were treated with cytokines for the indicated times and total RNA was analysed by northern blot for the gene encoding CAP. Representative results at 8 h of treatment are shown at the top. Densitometric analysis of CAP expression is shown below. **b**, Cytokine treatment inhibits troglitazone-induced histone acetylation and PPAR-γ DNA binding in the promoter of CAP. A ChIP assay[20] was done on cells treated with cytokines for 12 h. The PPRE-containing region (–1110 to –801) in the CAP promoter[19], the GRE-containing region (–528 to –110) in the PEPCK promoter or the C/EBP-RE-containing region (–361 to –73) in the PPAR-γ2 promoter[21] were amplified by PCR. Note that TNF-α and IL-1 inhibit the troglitazone-induced acetylation of histone H4 and the binding of PPAR-γ to the CAP promoter, clearly indicating that these cytokines inhibit the function of troglitazone-bound PPAR-γ on the PPRE. By contrast, no inhibition of the binding of GR or C/EBP-β to the target gene promoters was observed on cytokine treatment.

synthetic PPAR-γ ligands for the treatment of diabetes and the modulation of adipogenesis[23], we chose to investigate the effect of cytokines on PPAR-γ function.

Our results show that, of the signalling cascades downstream of TNF-α and IL-1, the TAK1/TAB1/NIK cascade suppresses PPAR-γ function by preventing PPAR-γ binding to DNA through an association with NF-κB that is coupled to the suppression of AF-1 function; this suggests that these cytokines reduce PPAR-γ function in pluripotent bone marrow stem cells, although the other signalling cascades[24] that activate NF-κB may also contribute to the PPAR-γ suppression. Together with studies showing that the activation of PPAR-γ signalling in the progenitor cells of lineage monocyte/macrophage inhibits osteoclastogenesis by suppressing NF-κB function[25], it is likely that the suppression of PPAR-γ function increases the sensitivity of stem cells to other cytodifferentiation factors, thereby inducing the development of cell types other than adipocytes, such as osteoblasts and osteoclasts[1,2,25].

In the nucleus, translocated NF-κB seems to interact directly both with the DNA-binding domain of PPAR-γ and with PGC-2 bound to AF-1 in the A/B domain of PPAR-γ, and the resultant complex blocks the binding of PPAR-γ/RXR-α heterodimers to target gene promoters. Because the functions of PPAR-γ AF-1 and PGC-2 have important roles in fat cell differentiation, this interaction with NF-κB may also interfere with their adipogenic functions. Although NF-κB is reported to associate with many other nuclear receptors, NF-κB seems to be recruited preferentially to PPAR-γ, at least in bone marrow stem cells, by its interaction with PGC-2, because the physical interaction of PGC-2 with PPAR-γ is highly selective among nuclear receptors[18]. Previous reports have shown that NF-κB function is inhibited by PPAR-γ ligands, including troglitazone, which act as anti-inflammatory agents[26,27]. It therefore seems that complexes formed by ligand-bound PPAR-γ, NF-κB and unknown factors lead to mutual inactivation of both classes of transcription regulatory factor, probably by suppressing their functions.

In this respect, it would be interesting to examine whether nuclear receptor co-repressors (for example, NCoR and SMRT) are included in this complex, because findings in NcoR knockout mice[28] have raised the possibility that such co-repressors are recruited to both ligand-bound PPAR-γ and to unliganded PPAR-γ and suppress transcription by associating with histone deacetylases[29], resulting in chromatin in an inactive state. The identification of other components in the PPAR-γ–NF-κB complexes would be of interest, because it would increase our understanding of coupled transcriptional regulation mediated by distinct classes of regulatory factor located in the same complex. □

Methods

Plasmid construction

We inserted full-length PPAR-γ cDNA or Flag–PGC-2 cDNA into pcDNA3 (Invitrogen, Carlsbad, CA)[13,18]. Full-length p50 and the p65 mutant cDNAs were inserted into pcDNA3 vectors (Invitrogen). TAK1, TAK1^{K63W}, TAB1, NIK, NIK$^{629-947}$, MKK3, MKK3KK, MKK6, MKK6KK, MKK7, IKK-α, IKK-β, IKK-α^{K44A}, IκB-α and IκB-α$^{32A/36A}$ have been described[7–9]. A PPRE (3 × acyl-CoA-PPRE), a glucocorticoid response element (GRE), a C/EBP response element (C/EBP-RE)[21] and an 8 × GAL4-binding element (17M8) were inserted into the luciferase pGL3-basic vector (Promega, Madison, WI) as reporter plasmids. The bacterial GST fusion protein expression vector for GST-bound fragments of PPAR (residues 1–506, 1–138, 1–203, 1–311, 204–506, 312–506 and 139–311) and PGC-2 (refs 13, 18) were inserted into the pGEX 4T-1 vector (Amersham Pharmacia, Piscataway, NJ). We generated RNAi constructs (NIK, +34 to +53; TAK1, +84 to +103; PGC-2, –14 +6) in an mU6-pro vector[30].

Cell culture

ST2 stromal cells derived from mouse bone marrow were cultured in α-MEM medium containing 10% fetal bovine serum (FBS) and treated with TNF-α (1 ng ml^{-1}), IL-1 (10 ng ml^{-1}), H_2O_2 (1 mM), troglitazone (1 μM), dexamethasone (0.1 μM), all-*trans* retinoic acid (10 nM) or combinations thereof. After 7 d, lipid accumulation was assessed by staining with Oil-Red-O to detect adipocytes. We derived NIK and NIK$^{629-947}$ stable transformants by transfecting the ST2 cell line. Primary cultured bone marrow cells were obtained from femoral and tibia cells of wild-type, PPAR-γ$^{+/-}$ or TNF-RI$^{-/-}$II$^{-/-}$ mice[5,12] by flushing with α-MEM, and contaminated red blood cells were haemolysed in 0.017 M Tris-HCl (pH 7.5) buffer containing 0.8% ammonium chloride. We rinsed cell suspensions in PBS twice and cultured them in α-MEM with 10% FBS at 37 °C.

Transfection and luciferase assay

Cells at 40–50% confluence were transfected in 12-well petri dishes by Lipofectamine regent (Gibco-BRL, Grand Island, NY). The total amount of DNA was adjusted to 1.0 μg by adding empty vector. We determined luciferase activity by using the Luciferase Assay System (Promega, Madison, WI). As a reference plasmid to normalize transfection efficiency, 25 ng of pRL-CMV plasmid (Promega) was co-transfected in all experiments[14,16].

Co-immunoprecipitation and western blotting

The transfected ST2 cells were washed twice in ice-cold PBS, collected, resuspended in 1 ml of ice-cold lysis buffer (10 mM Tris-HCl (pH 7.5), 1% Nonidet P-40, 0.15 M NaCl and 1 mM EDTA) and incubated for 30 min on ice. After centrifugation, supernatants were used as whole-cell extracts for immunoprecipitation with antibodies against either p50 or p65 (Santa Cruz Biotechnology, Santa Cruz, CA), followed by western blotting with antibodies specific for human PPAR-γ (H-100; Santa Cruz Biotechnology, Santa Cruz, CA)[14], GR (ABR, Golden, CO), Flag (anti-Flag monoclonal antibody; Sigma, St Louis, MI) or haemagglutinin A (HA; MBL, Nagoya, Japan).

Alkaline phosphatase staining

For histochemical staining of alkaline phosphatase[11], cells were fixed for 10 min with 3.7% formaldehyde at room temperature. After washing the cells in PBS, we incubated them for 20 min at room temperature with a mixture of 0.1 mg ml^{-1} naphthol AS-MX phosphate (Sigma), 0.5% *N,N*-dimethylformamide, 2 mM $MgCl_2$ and 0.6 mg ml^{-1} of fast blue BB salt (Sigma, St Louis, MI) in 0.1 M Tris-HCl (pH 8.5).

GST pull-down assay

Human PPAR-γ, PGC-2 and the deletion mutants were expressed as GST fusion proteins in *Escherichia coli* as described[13] and bound to glutathione-conjugated Sepharose 4B beads (Amersham Pharmacia). *In vitro* translated NF-κB proteins were incubated with the beads in NET-N buffer (0.5% Nonidet P-40, 20 mM Tris-HCl (pH 7.5), 200 mM NaCl, 1 mM EDTA) containing 1 mM phenyl methylsulphonyl fluoride. We separated the bound proteins by 7.5% SDS–PAGE, lightly stained them with Coomasie brilliant blue to verify equal amounts of fusion proteins and then visualized them by autoradiography.

EMSA

Nuclear extracts were prepared from transfected ST2 cells 30 min after cytokine treatment. Binding

reactions using acyl-CoA-PPRE as a DNA probe were done on ice for 30 min in binding buffer (10 mM HEPES (pH 7.9), 100 mM KCl, 7.5% glycerol, 1 mM dithiothreitol and 0.1% Nonidet P-40), 2 μg poly (dI-dC) and 10 μg of bovine serum albumin in a final volume of 25 μl. An antibody against PPAR-γ2 (ABR) was added to detect a supershift. Labelled PPRE DNA fragments were added to the binding mixtures, and further incubated for 20 min at room temperature. Whole reaction mixtures (25 μl) were loaded onto 5.0% polyacrylamide gels in Tris-acetate-EDTA buffer and separated by electrophoresis at 4 °C. We dried gels on filter paper and exposed them to X-ray film[17].

Northern blot analysis

Total cellular RNA was isolated from ST2 cells by Isogen (Wako, Osaka, Japan), and 20 μg of RNA was used for northern blot analysis with cDNAs for CAP, PPAR-γ, C/EBP-β, aP2, LPL, alkaline phosphatase, PGC-2 and glyceraldehyde-3-phosphate dehydrogenase (GAPDH) used as probes[17,18].

ChIP assay

We cultured ST2 cells for 2 d in the presence or absence of troglitazone or dexamethasone with or without cytokines and used the ChIP Assay Kit (Upstate Biotechnology, Lake Placid, NY) with an antibody[18] against acetylated histone H4, the H-100 antibody against human PPAR-γ, an antibody against GR antibody or antibodies against C/EBP-β (Santa Cruz Biotechnology, Santa Cruz, CA). For amplification by polymerase chain reaction (PCR), we used the primer pair 5′-GTCAACTTGACACAGGCTAA-3′ (−1110 to 1091) and 5′-TTAGACTTCCACAACGCTGCT-3′ (−819 to − 801) in the CAP gene promoter region for PPRE[26], 5′-GTAACACACCCCAGCTAACT-3′ (−528 to −509) and 5′-ATCATAGCCATGGTCAGCAC-3′ (−129 to −110) in the phosphoenolpyruvate carboxykinase (PEPCK) gene promoter region for GRE and 5′-GCCACTGGTGTG-TATTTTAC-3′ (−361 to −342) and 5′-CAAATATTTGGGAGAGGTGGG-3′ (−93 to −73) in the PPAR-γ2 gene promoter region for C/EBP-RE[21]. Optimal PCR conditions for semi-quantitative measurement were 24 cycles of 30 s at 96 °C, 15 s at 58 °C, and 1 min at 72 °C. PCR products were visualized on 2% agarose/Tris-Acetate-EDTA (TAE) gels[20].

RECEIVED 2 APRIL 2002; REVISED 9 NOVEMBER 2002; ACCEPTED 18 NOVEMBER 2003; PUBLISHED 24 FEBRUARY 2003.

1. Gimble, J. M. *et al.* Bone morphogenetic proteins inhibit adipocyte differentiation by bone marrow stromal cells. *J. Cell. Biochem.* 58, 393–402 (1995).
2. Ducy, P., Schinke, T. & Karsenty, G. The osteoblast: a sophisticated fibroblast under central surveillance. *Science* 289, 1501–1504 (2000).
3. Ron, D., Brasier, A. R., McGehee, R. J. & Habener, J. F. Tumor necrosis factor-induced reversal of adipocytic phenotype of 3T3-L1 cells is preceded by a loss of nuclear CCAAT/enhancer binding protein (C/EBP). *J. Clin. Invest.* 89, 223–233 (1992).
4. Torti, F. M., Torti, S. V., Larrick, J. W. & Ringold, G. M. Modulation of adipocyte differentiation by tumor necrosis factor and transforming growth factor β. *J. Cell. Biol.* 108, 1105–1113 (1989).
5. Kubota, N. *et al.* PPARγ mediates high-fat diet-induced adipocyte hypertrophy and insulin resistance. *Mol. Cell* 4, 597–609 (1999).
6. Takaesu, G. *et al.* TAB2, a novel adaptor protein, mediates activation of TAK1 MAPKKK by linking TAK1 to TRAF6 in the IL-1 signal transduction pathway. *Mol. Cell* 5, 649–658 (2000).
7. Ninomiya-Tsuji, J. *et al.* The kinase TAK1 can activate the NIK–IκB as well as the MAP kinase cascade in the IL-1 signalling pathway. *Nature* 398, 252–256 (1999).
8. Shirakabe, K. *et al.* TAK1 mediates the ceramide signalling to stress-activated protein kinase/c-Jun N-terminal kinase. *J. Biol. Chem.* 272, 8141–8144 (1997).
9. Shibuya, H. *et al.* TAB1: an activator of the TAK1 MAPKKK in TGF-β signal transduction. *Science* 272, 1179–1182 (1996).
10. Hu, E., Kim, J. B., Sarraf, P. & Spiegelman, B. M. Inhibition of adipogenesis through MAP kinase-mediated phosphorylation of PPARγ. *Science* 274, 2100–2103 (1996).
11. Yamaguchi, A., Komori, T., Suda, Regulation of osteoblast differentiation mediated by bone morphogenetic proteins, hedgehogs, and Cbfa1. Endocr. Rev. 21, 393–411 (2000).
12. Peschon, J. J. et al. TNF receptor-deficient mice reveal divergent roles for p55 and p75 in several models of inflammation. J. Immunol. 160, 943–952 (1998).
13. Kodera, Y. *et al.* Ligand type-specific interactions of peroxisome proliferator-activated receptor γ with transcriptional coactivators. *J. Biol. Chem.* 275, 33201–33204 (2000).
14. Yanagisawa, J. *et al.* Convergence of transforming growth factor-β and vitamin D signalling pathways on SMAD transcriptional coactivators. *Science* 283, 1317–1321 (1999).
15. Woronicz, J. D., Gao, X., Cao, Z., Rothe, M. & Goeddel, D. V. IkB kinase-b: NF-kB activation and complex formation with IkB kinase-a and NIK. Science 278, 866–869 (1997).
16. Kato, S. et al. Activation of the estrogen receptor through phosphorylation by mitogen-activated protein kinase. Science 270, 1491–1494 (1995).
17. Chen, F. E., Huang, D. B., Chen Y. O. & Ghosh, G. Crystal structure of p50/p65 heterodimer of transcription factor NF-kB bound to DNA. Nature 391, 410–413 (1998).
18. Castillo, G. et al. An adipogenic cofactor bound by the differentiation domain of PPARg. EMBO J. 13, 3676–3687 (1999).
19. Baumann, C. A., Chokshi, N., Saltiel, A. R. & Ribon, V. Cloning and characterization of a functional peroxisome proliferator activator receptor-gamma-responsive element in the promoter of the CAP gene. *J. Biol. Chem.* 275, 9131–9135 (2000).
20. Chen, H., Lin, R. J., Xie, W., Wilpitz, D. & Evans, R. M. Regulation of hormone-induced histone hyperacetylation and gene activation via acetylation of an acetylase. *Cell* 98, 675–86 (1999).
21. Zhu, Y. et al. Structural organization of mouse peroxisome proliferator-activated receptor g (mPPARg) gene: alternative promoter use and different splicing yield two mPPAR g isoforms. Proc. Natl Acad. Sci. USA 17, 7921–7925 (1995).
22. Teitelbaum, S. L. Bone resorption by osteoclasts. *Science* 289, 1504–1508 (2000).
23. Kersten, S., Desvergne, B. & Wahli, W. Roles of PPARs in health and disease. *Nature* 405, 421–424 (2000).
24. Wajant, H., Henkler, F. & Scheurich, P. The TNF-receptor-associated factor family: scaffold molecules for cytokine receptors, kinases and their regulators. Cell Signal 13, 389–400 (2001).
25. Mbalaviele, G. et al. Activation of peroxisome proliferator-activated receptor-g pathway inhibits osteoclast differentiation. J. Biol. Chem. 275, 14388–14393 (2000).
26. Ricote, M., Li, A. C., Willson, T. M., Kelly, C. J. & Glass, C. K. The peroxisome proliferator-activated receptor-g is a negative regulator of macrophage activation. Nature 391, 79–82 (1998).
27. Rossi, A. *et al.* Anti-inflammatory cyclopentenone prostaglandins are direct inhibitors of IκB kinase. *Nature* 403, 103–108 (2000).
28. Jepsen, K. *et al.* Combinatorial roles of the nuclear receptor corepressor in transcription and development. *Cell* 102, 753–763 (2000).
29. Glass, C. K. & Rosenfeld, M. G. The coregulator exchange in transcriptional functions of nuclear receptors. *Genes Dev.* 14, 121–141 (2000).
30. Yu, J. Y., DeRuiter, S. L. & Turner, D. L. RNA interference by expression of short-interfering RNAs and hairpin RNAs in mammalian cells. Proc. Natl Acad. Sci. USA 99, 6047–6052 (2002).

ACKNOWLEDGEMENTS

We thank S. Tanaka for discussions; R. Nakamura and H. Higuchi for manuscript preparation; Sankyo Pharmaceuticals for troglitazone; P. Chambon for the mouse RXR-α cDNA; and D. Turner for the RNAi vector. This work was supported in part by a Grant-in-Aid for Priority Areas from the Ministry of Education, Science, Sports and Culture of Japan (to S.K.).

Correspondence and requests for materials should be addressed to S.K.

COMPETING FINANCIAL INTERESTS

The authors declare that they have no competing financial interests.

0013-7227/04/$15.00/0
Printed in U.S.A.

Endocrinology 145(4):1860–1869

doi: 10.1210/en.2003-1182

A Benzimidazole Fungicide, Benomyl, and Its Metabolite, Carbendazim, Induce Aromatase Activity in a Human Ovarian Granulose-Like Tumor Cell Line (KGN)

HIDETAKA MORINAGA, TOSHIHIKO YANASE, MASATOSHI NOMURA, TAIJIRO OKABE, KIMINOBU GOTO, NOBUHIRO HARADA, HAJIME NAWATA

Department of Medicine and Bioregulatory Science (Third Department of Internal Medicine), Graduate School of Medical Sciences, Kyushu University (H.M., T.Y., M.N., T.O., K.G., H.N.), Higashi-ku, Fukuoka 812-8582, Japan; Core Research for Evolutional Science and Technology, Japan Science and Technology Corp. (H.M., T.Y., M.N., T.O., K.G., H.N.), Kawaguchi, Saitama 332-0012, Japan; and Department of Biochemistry, Fujita Health University School of Medicine (N.H.), Toyoake, Aichi 470-1192, Japan

Endocrine disruptor chemicals are known to cause a range of abnormalities in sexual differentiation and reproduction. One mechanism underlying such effects may be via alteration of aromatase activity, which is responsible for estrogen production. A good screening system for identifying endocrine disruptors has long been desired. We have recently established a human ovarian granulosa-like tumor cell line, KGN, which possesses a relatively high level of aromatase expression and is considered a useful mammalian model for investigating the *in vitro* effects of various chemicals on aromatase activity. In this study we screened 55 different candidate chemicals for endocrine disruptors by assaying aromatase activity. Only benomyl, known as both a benzimidazole fungicide and a microtubule-interfering agent, was found to induce aromatase activity in association with increased levels of aromatase mRNA in KGN cells. The effect of benomyl was presumed to be mediated by its metabolite carbendazim, because it produced an effect equivalent to that of benomyl. The mechanism underlying the benomyl-induced increase in aromatase activity appears independent of the cAMP-protein kinase A pathway. Treatment with taxol, another class of microtubule-interfering agents, also caused induction of aromatase in KGN cells. Both benomyl and taxol changed KGN cell morphology, including the development of cell roundness and a disorganized network of microtubules. These results indicate that benomyl is a potential endocrine disruptor that provides a novel estrogenicity and operates through a microtubule-interfering mechanism. (*Endocrinology* 145: 1860–1869, 2004)

THERE ARE SERIOUS concerns that certain environmental contaminants and commercial products have the potential to disturb endocrine function in humans and wildlife, lead to impaired reproductive capacity, and have other toxic effects on sexual differentiation, growth, and development (1, 2). These chemicals are called endocrine disruptors and act as estrogenic or antiestrogenic agents by affecting both the synthesis and the action of estrogen. Many chemicals exert their effects by blocking or activating steroid hormone receptors and/or affecting the levels of sex hormones. These effects can disrupt the development or differentiation of both the male and the female reproductive system. These facts emphasize the importance of screening candidate chemicals for a wide range of hormone-mimicking effects.

One important enzyme in the steroid synthesis pathway is cytochrome P450 aromatase (aromatase), which is a product of the *CYP19* gene and catalyzes the rate-limiting step in the conversion of androgens into estrogens. Aromatase is responsible for maintaining the homeostatic balance between androgens and estrogens in both sexes. This enzyme is expressed by many human tissues, including the ovary, testis, placenta, brain, liver, adipose, muscle, and breast tissue. This pattern of aromatase expression is regulated by a tissue-specific promoter derived from alternative splicing of the *CYP19* gene (3, 4).

For several years the activating or inhibiting effects of some endocrine disruptors on aromatase activity have been reported. Aromatase activity can be induced by 2-chloro-*s*-triazine herbicide (atrazine, simazine, and propazine) *in vitro* (5) and by *p,p'*-dichlorodiphenyldichloroethane (*p,p'*-DDE) *in vitro* and *in vivo* (6). Recently, we demonstrated that tributyltin and triphenyltin, commonly used as biocides in antifouling paint and wood preservatives, inhibited aromatase activity *in vitro* (7). Also, several chemicals, including pesticides such as prochloraz, fenarimol, triadimefon, triadimenol, and mono-(2-ethylhexyl) phthalate, suppress aromatase activity *in vitro* (8–12).

We have recently established a steroidogenic human ovarian granulosa-like tumor cell line, KGN, from a patient with invasive granulosa cell carcinoma (13). The cell line possesses properties similar to those of normal granulosa cells, including relatively high aromatase activity. The cell line is thus considered to be a useful model for investigating the effects

Abbreviations: CRE, cAMP-responsive element; DMSO, dimethylsulfoxide; hMG, human menopausal gonadotropin; MIA, microtubule-interfering agent; PI3 kinase, phosphatidylinositol-3OH-kinase; PKA, protein kinase A; PKB, protein kinase B; *p,p'*-DDD, *p,p'*-dichlorodiphenyldichloroethane; P450scc, cytochrome P450 side-chain cleavage; Sgk, serum and glucocorticoid-induced kinase; StAR, steroidogenic acute regulatory protein.

Endocrinology is published monthly by The Endocrine Society (http://www.endo-society.org), the foremost professional society serving the endocrine community.

of some endocrine disruptors on aromatase activity *in vitro* (7). Using this system, we screened 55 candidate chemicals for endocrine disruption in assays of aromatase activity and found that only benomyl [methyl 1-(butylcarbamoyl)-2-benzimidazolecarbamate], a benzimidazole fungicide commonly used on a variety of food crops and ornamental plants, induces aromatase activity in KGN cells. Benomyl is also able to interfere with the assembly of fungal microtubules (14), can rapidly degrade into carbendazim in aqueous (15) or organic (16) solutions, or as a result of hydroxylation in the microsomal monooxygenase system (17). In this study we investigated some of the mechanisms involved in benomyl-induced aromatase activity in association with the properties stated above.

Materials and Methods

Reagents and supplies

Chemicals were obtained from Wako Pure Chemical Co. (Osaka, Japan) and AccuStandard, Inc. (New Haven, CT). Carbendazim was obtained from Aldrich Chemical Co., Inc. (Milwaukee, WI). [1β-^{3}H]Androstenedione was obtained from NEN Life Science Products (Boston, MA). Wortmannin, U0126, PD98059, genistein, AG490, and AG1478 were obtained from Sigma-Aldrich Corp. (St. Louis, MO).

Cell culture

KGN cells were maintained in a DMEM/Ham's F-12 medium (Invitrogen, Grand Island, NY) supplemented with 10% FCS, penicillin (100 U/ml), and streptomycin (100 μg/ml) as previously described (13).

Human ovarian granulosa cells were obtained from four women who underwent *in vitro* fertilization. Written informed consent was obtained from each subject before the study. The brief protocol of *in vitro* fertilization was described previously (18). Granulosa cells were plated on a 24-well plate (Nulge, Nunc International, Naperville, IL) and cultured as previously described (18).

Aromatase assay

Aromatase activity was determined by measuring the amount of [^{3}H]H_2O released with the conversion of [1β-^{3}H]androstenedione into estrone as described previously (13). Briefly, the cells were cultured in a 24-well dish in DMEM/Ham's F-12 with 10% FCS in the presence or absence of various chemicals and incubated for 24 h. The cells were then incubated with [1β-^{3}H]androstenedione for an additional 6 h. The medium was extracted with chloroform and centrifuged. The aqueous phase was then mixed with 5% charcoal/0.5% dextran and incubated for 30 min. The mixture was subsequently centrifuged, and the supernatant was added to 5 ml scintillation fluid and assayed for radioactivity. The amount of radioactivity in [^{3}H]H_2O was standardized from the protein concentration determined using a protein assay kit (Bio-Rad Laboratories, Hercules, CA).

Measurement of cAMP and progesterone

The cAMP content in the cell culture medium, incubated with various chemicals, was measured by RIA using a commercially available kit (Yamasa Syoyu Co. Ltd., Chiba, Japan) (19). The content of progesterone in the medium was also measured by a specific RIA (SRL, Tokyo, Japan).

Luciferase assay and transfection

KGN cells were transfected using SuperFect transfection reagent (Qiagen, Hilden, Germany) with the pGL3-basic luciferase reporter plasmid (Promega Corp., Madison, WI) that contains 4 kb *CYP19* promoter II (20) or cAMP-responsive element (CRE) plasmid-luciferase (Clontech Laboratories, Palo Alto, CA) plasmid, which contains two copies of the CRE consensus sequence (TGACGTCA). The *Renilla* luciferase control reporter plasmid phRG-TK was used as an internal control for transfection efficiency. Luciferase assays were performed in the cell lysate by treating the luciferase lysis buffer with a dual luciferase reporter assay system (Promega Corp.). Luminescence activity was measured with a LUMAT LB9507 luminometer (Berthold Technologies GmbH & Co., Bad Wildbad, Germany).

RNA extraction, semiquantitative RT-PCR, and quantitative real-time PCR

KGN cells were cultured in the presence or absence of various chemicals. After 24 h of culture, total RNA was extracted with ISOGEN (Wako Pure Chemical Co.) and stored at −80 C for later analysis. The extracted RNA was subjected to a reverse transcriptase reaction using Superscript II (Invitrogen). The oligonucleotides used for PCR were custom-ordered from Hokkaido System Science Co. Ltd. (Sapporo, Japan). First-strand cDNA was synthesized using 5 μg total RNA as a template. PCR carried out with T-Gradient Thermoblock (Biometra Biomedizinische Analytik GmbH, Gottingen, Germany). The sense/antisense primers used were: aromatase, 5′-GGTCACAGTCTGTGCTGAATCC-3′/5′-ACTCGAGTC TGTGCATCCTTAA-3′; cytochrome P450 side-chain cleavage (P450scc), 5′-GAGATCCCCTCTCCTGGTGA-3′/5′-TGGCGCTCCCCAAAAATGA-3′; steroidogenic acute regulatory protein (StAR), 5′-GCAGCAG-CAGCGGCGGCA-3′/5′-TGTGTCCATGCCAGCCAGC-3′; and β-actin, 5′-TCGTGCGTGACATTAAGGAG-3′/5′-GATGTCCACGTCACACTT CA-3′. Based on preliminary experiments, to achieve linear amplification, the PCRs for aromatase, P450scc, StAR, and cDNA were performed in 35, 30, and 30 cycles, respectively, whereas that for β-actin cDNA was performed in 28 cycles. Each PCR amplification for aromatase, P450scc, StAR, and β-actin was started by an initial denaturing reaction at 94 C for 5 min, followed by 35, 30, 30, and 28 cycles of denaturing (30 sec, 94 C) and elongation (1 min, 72 C) reactions, respectively. Annealing was performed for 30 sec at 60 C for aromatase, 50 C for P450scc, 48 C for StAR, and 60 C for β-actin, respectively. The PCR products were visualized by electrophoresis on a 1.5–2.0% agarose gel containing 0.5 mg/ml ethidium bromide and luminescence was measured by NIH image. We finally verified the nucleotide sequence of each PCR product by direct sequencing using the appropriate primers.

To reconfirm the relatively small increase in aromatase mRNA by benomyl obtained by RT-PCR analysis, we also performed a quantitative real-time PCR. First-strand cDNA was synthesized using 5 μg total RNA as a template. The sense/antisense primers for real-time PCR were the same as those used in RT-PCR, except for aromatase (5′-ACGCA-GGATTTCCACAGAAGAG-3′/5′-CTTCTAAGGCTTTGCGCATGAC-3′) and glyceraldehyde-3-phosphate dehydrogenase (5′-CCACCCATGGCA-AATTCCATGGCA-3′/5′-TCTAGACGGCAGGTCAGGTCCACC-3′). PCR was carried out with a LightCycler (Roche Diagnostics GmbH, Mannheim, Germany) according to the manufacturer's instructions. Briefly, 1 μl cDNA (or H_2O control) was placed into a 20-μl reaction volume containing 1 μl of each primer and 2 μl LightCycler-FastStart DNA Master SYBR Green I (Roche, Mannheim, Germany). Nucleotides, *Taq* DNA polymerase, and buffer were included in the LightCycler-FastStart DNA Master SYBR Green I. The thermal cycling conditions comprised an initial denaturation step at 95 C (10 min), followed by 40 cycles of 95 C (0 sec), 63 C (15 sec), and 72 C (40 sec). Threshold values were obtained where fluorescent intensity was in the geometric phase of amplification, as determined via LightCycler software version 3.5. Products were verified on a 2% agarose gel.

Western blotting

Cell lysates were prepared by treating cells with CelLytic-M (Sigma-Aldrich Corp.) containing protease inhibitor. Lysate was sonicated for 20 sec on ice and centrifuged at 10,000 × *g* for 10 min to separate the particulate materials. SDS-PAGE was performed under reducing conditions on 10% polyacrylamide gels. The resolved proteins were transferred onto a polyvinylidene difluoride membrane (Amersham Pharmacia Biotech, Piscataway, NJ) and then incubated with rabbit antiserum raised against human aromatase (1:1000) (21). After several washes with PBS, the membrane was incubated with the secondary antibody to IgG conjugated with horseradish peroxidase (1:2000). The blots were then probed with the ECL$^+$ Western blot detection system (Amersham Pharmacia Biotech) in accordance with the manufacturer's instructions.

Immunofluorescence microscopy

KGN cells were seeded in the chambers of a two-well glass slide (Nulge, Nunc International). After drug treatments and incubation, the growth medium was removed and then immediately fixed with 4% paraformaldehyde for 30 min. Cells were permeabilized using 0.2% Triton X-100 in PBS for 10 min at room temperature and then incubated with blocking buffer (Block Ace, Dainippon Pharmaceutical Co. Ltd., Osaka, Japan) for 1 h. Anti-α-tubulin (Molecular Probes, Eugene, OR) diluted 1:200 with 10% Block Ace in PBS was added to the samples for 1 h at room temperature. Samples were then washed three times with PBS, and Alexa Fluor 488 goat antimouse (Molecular Probes) antibodies diluted 1:1000 with 10% Block Ace in PBS was applied to the samples for 1 h at room temperature. Samples were mounted in ProLong Antifade Mounting Media (Molecular Probes) for preservation and observation. Images were collected using a fluorescent microscope (Olympus Optical Co. Ltd., Tokyo, Japan) and a High Sensitive CCD camera (Keyence Corp., Osaka, Japan).

Statistics

All experiments were carried out at least three times, with triplicate plates per point. All values represent the mean ± SD. A one-way ANOVA was used for statistical evaluation. $P < 0.05$ indicated statistical significance.

Results

Screening of endocrine disruptor chemicals for aromatase activity in KGN cells

We obtained 55 chemicals that may act as endocrine disruptor chemicals and examined the effects of these chemicals, at a concentration of 10^{-5} M (except for 10^{-7} M tributyltin and 10^{-7} M triphenyltin), on aromatase activity in KGN cells. Only benomyl was found to induce aromatase activity (Fig. 1A). At a concentration of 10^{-5} M, benomyl induced a remarkable 3-fold increase in aromatase activity compared with the dimethylsulfoxide (DMSO) control. Benzo(a)pyrene and heptachlor also caused a slight, but significant, increase in aromatase activity, whereas heptachlor, *p,p'*-DDD, *p,p'*-DDE, cyper-

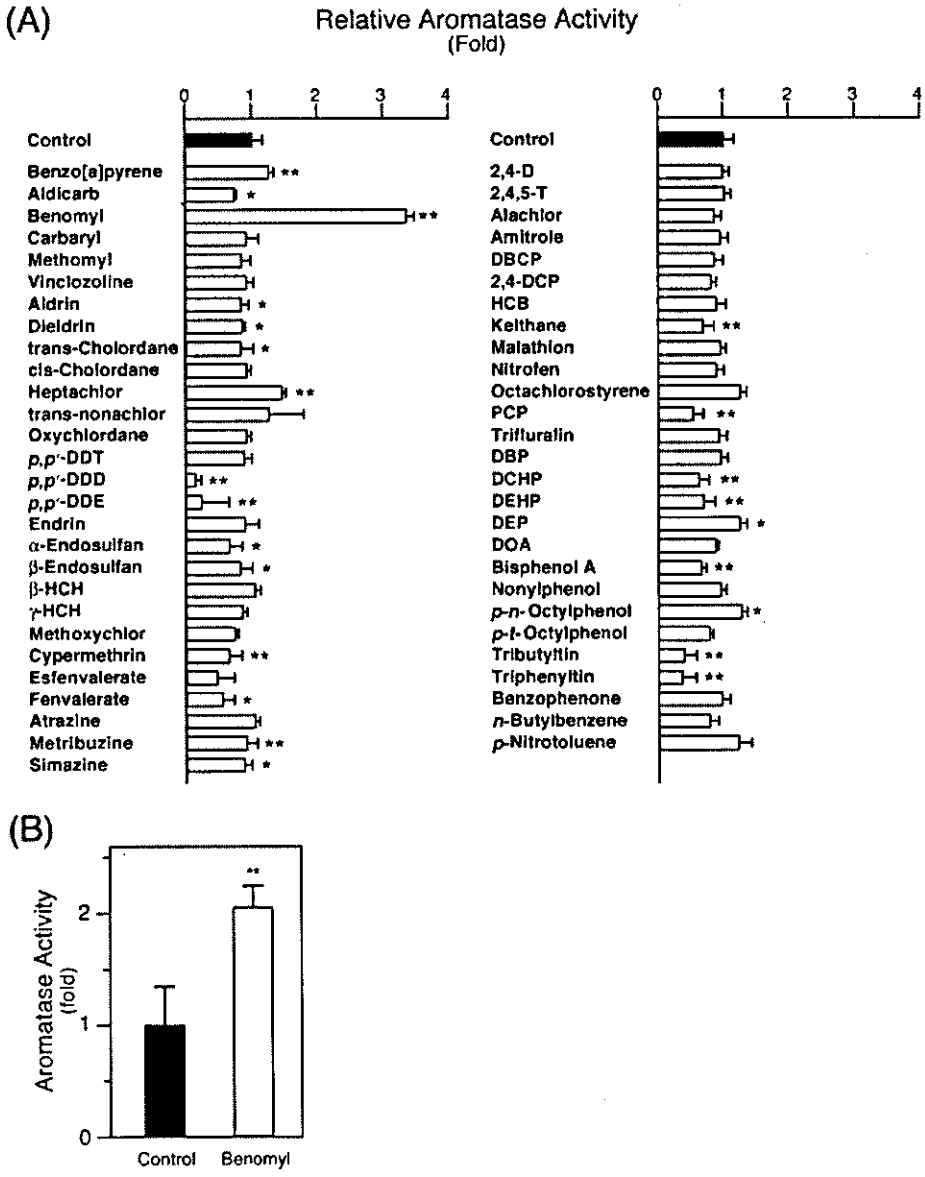

FIG. 1. Screening of 55 endocrine disruptor chemicals for aromatase activity in cultured KGN cells. A, KGN cells were cultured and 10^{-5} M of each compound (except for 10^{-7} M tributylin and 10^{-7} M triphenyltin) or DMSO (control) was added to the medium, incubation was performed for 24 h, and aromatase activity was assayed as described in *Materials and Methods*. B, Normal granulosa cells were cultured in the presence or absence of 10^{-5} M benomyl, and aromatase activity was assayed as described in *Materials and Methods*. Each value indicates the mean ± SD of three experiments, with triplicate plates per point. *, $P < 0.05$; **, $P < 0.01$ (*vs.* control).